Fall 12-20-2017

Line Start Permanent Magnet Synchronous Motor for Multi Speed Application

Bikrant Poudel
bpoudel2@uno.edu

Line Start Permanent Magnet Synchronous Motor for Multi Speed Application

A Thesis

Submitted to the Graduate Faculty of the
University of New Orleans
in partial fulfillment of the
requirement for the degree of

Master of Science
In
Electrical Engineering

By

Bikrant Poudel

B.S. Tribhuvan University, 2013

December 2017

Acknowledgement

To my parents, my lovely wife Jyoti and my sisters, who always pushed me to take one more step, deepest thanks, I owe it all to you.

My most sincere thanks to my advisor, mentor and professor Dr. Ebrahim Amiri for accepting me as his student and guiding through my master's studies.

Word of thanks to Dr. Parviz Rastgoufard and Dr. Ittiphong Leevongwat for their encouragement and knowledge they have conferred upon me.

A special thanks to my friends Rochak, Nirdesh and Manisha.

Finally, word of thanks to all the faculty of Electrical Engineering Department, University of New Orleans who have help me learn new things.

Thank you all for your encouragement.

Contents

List of Figures

List of Tables

Abstract

This thesis aims to design and develop line start permanent magnet synchronous motors capable of operating in two distant synchronous speeds with good starting torque and steady state characteristics for variety of industrial applications, such as fan and offshore crane. The proposed designs are based on variable pole numbers for the stator and the rotor. The stator winding consist of two independent windings with different pole numbers to switch the winding and change the operating pole count for low and high speed applications. For the motor to operate in these two distinct operating speeds, the rotor must be capable of creating two different magnetic polarities (pole numbers) to adapt itself to the stator operating pole number. For this purpose, two different schemes for the rotor structure are proposed. In scheme I two-speed operation is realized by the combination of electromagnetic torque and reluctance torque which enables the motor to operate as a synchronous PM motor at high speed and synchronous reluctance motor at low speed. In scheme II, rotor with dual PM polarity is proposed which enables the motor to operate as a PM motor at both low and high speed regions.

Keywords: LSPM Motor, PM Torque, Reluctance Torque, Multi-Speed Motor

Chapter 1

Introduction

Line Start Permanent Magnet (LSPM) motors are potentially an effective alternative to induction motors as they can operate with substantially higher efficiency and higher power factor. In addition, LSPM motors do not require inverters reducing the drive cost in comparison with other types of permanent magnet (PM) motors such PM brushless DC motor. Despite the advantages of LSPM motors, they suffer from poor starting torque and synchronization capability [1] and their operation is restricted to a single operating speed due to the fixed polarity of PM poles in the rotor. This has limited the implementation of LSPM motors for applications that require two or more operating speeds such as fans, pumps and offshore cranes.

Despite an improvement in starting and steady state performance (efficiency, power factor, and synchronous torque) of the motor [1-9], the existing technology on multi-speed synchronous motor still requires the power electronic driver unit [10-14]. Reference [14] proposed a design for the two-speed LSPM but the motor operates as an induction motor at high speed region (2-pole mode) and it is only at low speed (4-pole mode) that the motor can operate as PM motor.

This thesis presents two different schemes of line start permanent magnet synchronous motor capable of operating in two different speeds without requiring a drive unit. The first scheme proposed is based on variable pole numbers for the stator and the rotor. PMs are specially arranged so that the rotor contains a 4-pole PM configuration overlaid on an 8-pole reluctance configuration, with the stator windings being reconfigured by two separate windings to change the operating pole count. The second scheme proposed presents design of two-speed LSPM synchronous motor based on the rotor with dual magnetic polarity. PMs are specially arranged so that the rotor contains a 4-

pole PM configuration overlaid on an 8-pole PM configuration. This concept can be generalized to any pole number m and n.

1.1 Objective of Thesis

- Design of multi-speed LSPM motor with variable pole number.
- Comprehensive transient and steady state analysis of the motor under different load conditions using 3-D FEA

1.2 Tasks to Be Done

- To build 3-D motor models for scheme I and scheme II model in FEM using Ansoft Maxwel V16 software. Design Steps include:
    - Stator modeling
        - Stator Core Modeling
        - Winding Design for 4-pole and 8-pole configuration
    - Rotor modeling
        - Rotor Core Modeling
        - Permanent magnet placement
        - Squirrel cage design and placement
- To determine the flux density distribution.
- To perform steady state analysis including
    - Back EMF generation
    - Synchronous torque Vs. power angle response
- To excite the windings with 3-phase ac line voltage and perform
    - Transient speed analysis

- Transient Torque Analysis
- Transient Input phase current analysis
- Transient speed analysis for different moment of inertia of rotor.
- Transient speed analysis for different starting load torque.

- To find efficiency at different lamination factor.

1.3 Outline of Thesis

Chapter 1 presents the Introduction

Chapter 2 covers the overview of conventional synchronous motors.

Chapter 3 presents LSPM synchronous motor modelling in FEM.

Chapter 4 covers principle of operation, design, modeling, steady state and transient simulation and results of two speed LSPM synchronous motors

Chapter 5 presents the conclusion and future scope of the study.

Chapter 2

Overview of Conventional Synchronous Machines

Synchronous machines are the class of Alternating Current (AC) rotating machines. In such machines the speed of rotation under steady state condition is proportional to the frequency of current in the armature [15-23]. The speed of rotation of the magnetic field created by the armature current is same as the speed of the rotation of the magnetic field created by the field current of rotor [15-23]. The rotating speed is the synchronous speed hence the machines are called synchronous machines. Synchronous machines can either be used as generators or motors. In the synchronous machines the frequency of voltage in stator and rotor RPM relates as shown in (1) [22- 23].

$$n_s = \frac{120 * f}{p} \tag{1}$$

Where, n_S = synchronous speed in RPM

f = frequency of stator current

p = number of poles in stator

2.1 Synchronous Machine Construction

Synchronous machines consist two mechanical parts: a rotor and a stator and two electrical parts: an armature winding and a field source [22-23]. For a synchronous machine the field source is located at the rotor whereas the armature winding is located at the stator [22-23]. Conventionally the stator winding/ armature windings are three phase. The field winding DC excited or the rotor can also be constructed using PMs. The rotor can also be cylindrical as well as salient pole in nature [22-23]. Cylindrical rotor has one distributed winding and a uniform air gap, whereas the

salient pole rotors have concentrated windings and non-uniform air gap. Fig. 1 shows synchronous machines with cylindrical rotor and salient pole rotor respectively [22-23].

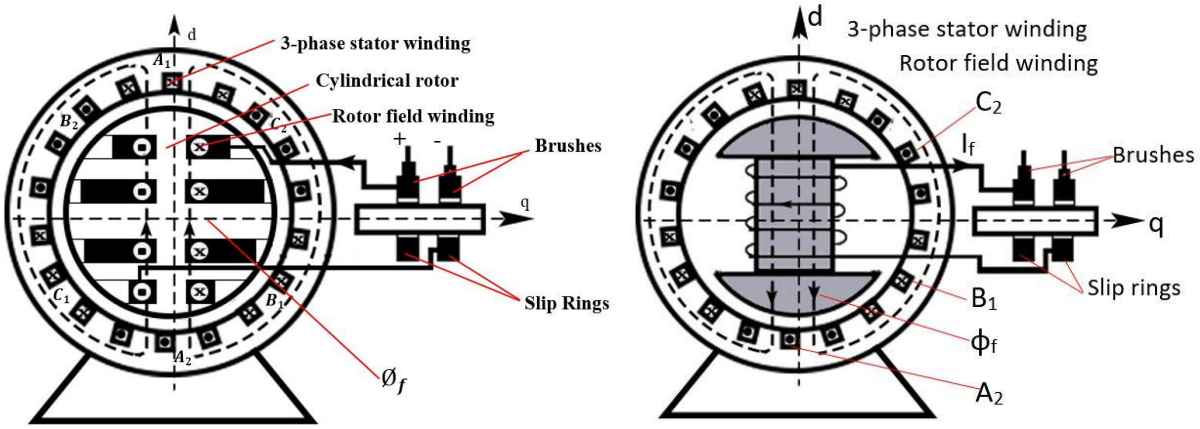

(a) (b)

Fig. 1. Construction of synchronous machines with: (a) Cylindrical Pole (b) Salient Pole

2.2 Angle in Electrical and Mechanical Units

For a synchronous machine the idealized radial distribution of the air gap flux density is sinusoidal along the air gap [22-23]. For a machine with two poles when the rotor makes a complete rotation the induced electromotive force (emf) which is sinusoidal also rotates by 360^o. Now, if we measure the rotor angle by mechanical degrees θ_m and phase angles of flux density and emf as electrical angle θ [22-23].

$$\theta = \theta_m \text{ for 2 pole motors} \quad (2)$$

But in case of four pole machines the relation is:

$$\theta = 2\theta_m \text{ for 4 pole motors} \quad (3)$$

Fig. 2 shows the rotor configuration for 2-pole and 4-pole configuration and Fig. 3 shows flux distribution/ emf in air gap for 2-pole and 4-pole rotor configuration respectively.

For general case, for a machine having P poles the relation between electrical angle and mechanical angle can be expressed as [22-23]

$$\theta = \frac{P}{2}\theta_m \tag{4}$$

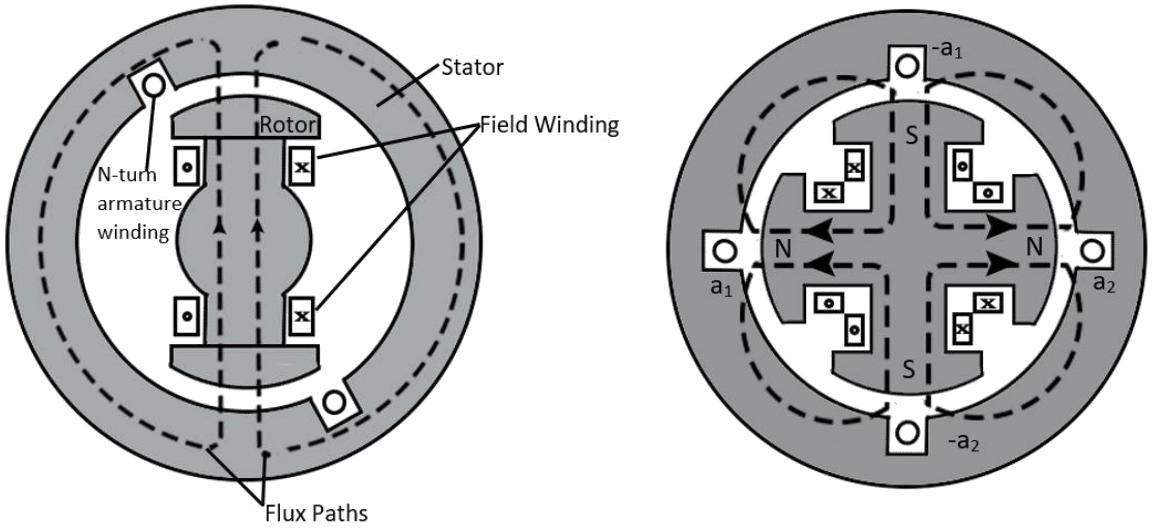

(a) (b)

Fig. 2. Synchronous machine (a) two pole and (b) four pole

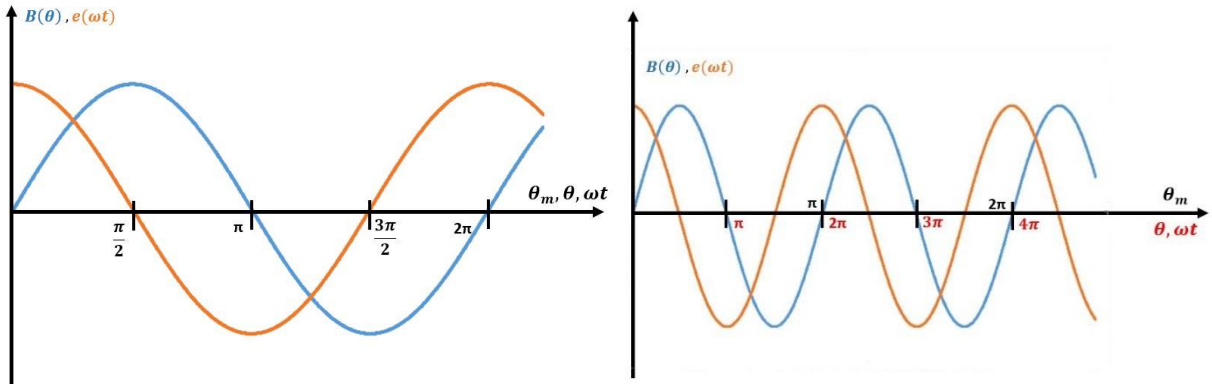

(a) (b)

Fig. 3. Flux density distribution in air gap and induced *emf* in the phase winding of a (a) two pole and (b) four pole synchronous machine

2.3 Synchronous Motor

As the name suggests the speed of rotor and the magnetic field created on the stator are the same in case of synchronous motor. Synchronous motors are fixed speed motors [22-23]. Equation 1 shows the relationship among frequency of voltage supplied at stator, number of poles of motor and RPM of motor. In synchronous motor the stator winding also known as armature winding is supplied with three phase AC voltage whereas the rotor winding also known as field winding is supplied with Direct Current (DC) voltage [22-23]. Construction of synchronous motors is as shown in Fig. 1. In synchronous motors the three phases of the armature windings are connected to three phase AC supply. The stator connected to three phase AC voltage produces the rotation magnetic flux whereas the field winding connected to a DC source produces the magnetic flux which is steady with respect to the rotor [22-23]. For the generation of torque these two magnetic field should rotate in synchronization meaning the rotor should rotate at the speed equal to the speed of rotating magnetic field on stator. For a synchronous motor the rotor follows the stators rotating field by an angle (-δ) also known as power angle. Fig. 4 shows the power angle δ where $\emptyset_a$ and $\emptyset_f$ are armature flux component and field flux component respectively [22-23]. Similarly ω_s represents the speed of motor.

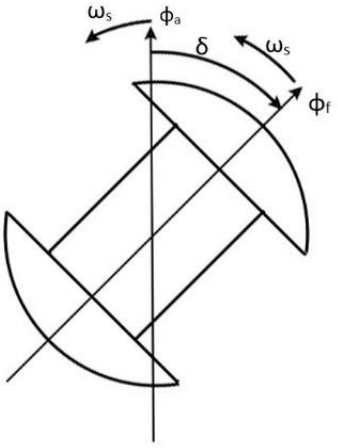

Fig. 4. Power angle between stator field and rotor field in synchronous motor

2.4 Electromagnetic power and torque of Synchronous motor

A synchronous machine when operated as a motor to drive any mechanical load needs to balance the load torque and the loss torque due to friction and windage in steady state, i.e.

$$T_{em} = T_{load} + T_{loss} \tag{5}$$

Since we define power as product of motor speed and motor torque we can express above equation by multiplying both sides with synchronous speed ω_s as follows

$$P_{em} = P_{load} + P_{loss} \tag{6}$$

Where, $P_{em} = T_{em}\omega_s$, $P_{load} = T_{load}\omega_s$ and $P_{loss} = T_{loss}\omega_s$ are electromagnetic power, mechanical power delivered to load and mechanical power loss of the system respectively. For a synchronous generator the conversion between the mechanical power and electrical power is shown as [22-23]

$$P_{em} = 3E_a I_a \cos \phi_{E_a I_a} = T_{em}\omega_s \tag{7}$$

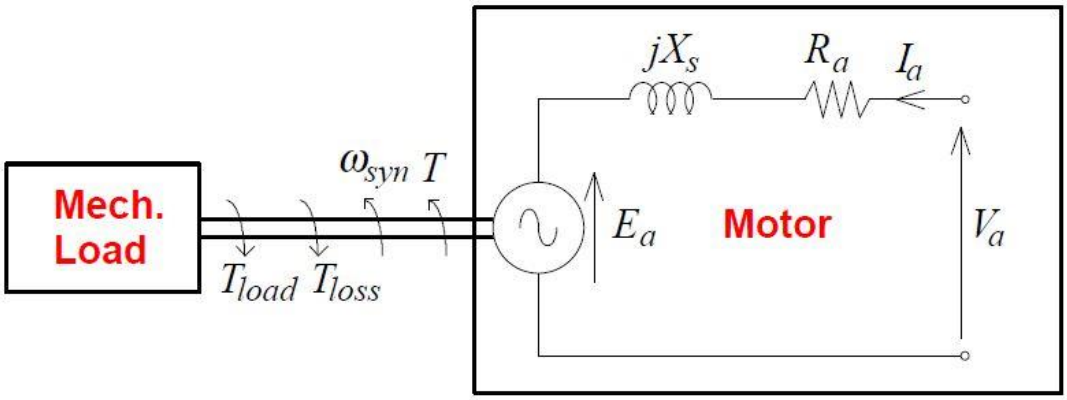

Fig. 5. Electrical equivalent of Synchronous motor

Where E_a, I_a and $\phi_{E_a I_a}$ are back emf, field current and angle between phasor E_a and I_a respectively.

Now ignoring the stator resistance per phase voltage can be expressed as:

$$V_a = E_a + jX_s I_a \tag{8}$$

Now using the phasor shown in Fig. 6 we can derive

$$V_a \sin\ (d) = X_s I_a \cos \phi_{E_a I_a} \text{ , where } \phi_{E_a I_a} = c - d \tag{9}$$

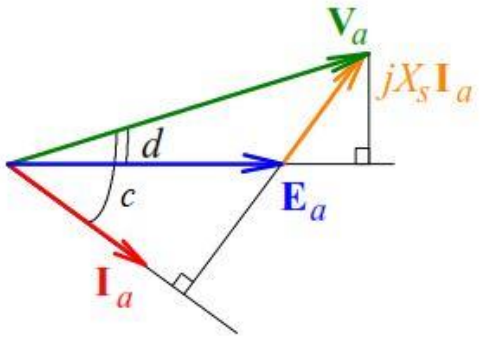

Fig. 6. Motor phasor diagram

Hence we can derive

$$P_{em} = \frac{3E_a V_a}{2X_s} \sin \delta \tag{10}$$

Also,

$$T = \frac{P_{em}}{\omega_s} = \frac{3E_a V_a}{2\omega_s X_s} \sin \delta \tag{11}$$

Where,

$p_{em} =$ number of poles

$\omega_s =$ synchronous angular velocity

$E_a =$ no load back EMF generated by the PMs

$X_s =$ reactance at the synchronous frequency

$V_a =$ input voltage

$\delta =$ torque angle

Where δ is the power angle. The power angle is negative for motor action. The torque-power angle characteristics at constant V and I_f is shown in Fig. 7 [22-23].

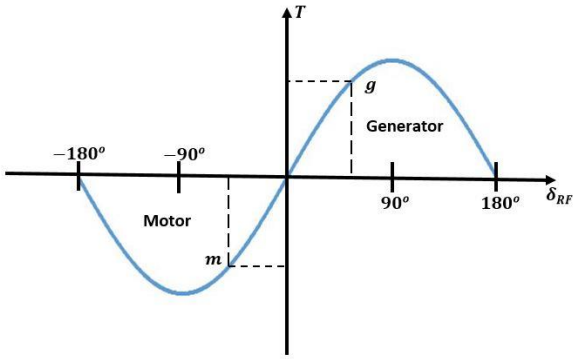

Fig. 7. Torque –power angle characteristics

2.5 Salient Pole Synchronous Motor

Salient pole rotors of synchronous motors have non-uniform air gap. This difference in air gap creates a difference in reluctance of the magnetic circuit which creates a torque known as reluctance torque [22-23]. The torque varies as a function of angular position of the rotor with respect to the stator. Magnetic reluctance is low along the pole shoe ($d-axis$) whereas it's maximum along the interpolar regions ($q-axis$) as shown in the Fig. 8 [22-23]. Assuming that a salient pole rotor of synchronous motor is under the influence of rotating stator field, the salient pole rotor will try to align itself in a direction of minimum reluctance. As the stator field rotates this tendency of alignment of the rotor causes the rotor to move at a speed equal to speed of rotation of stator magnetic field.

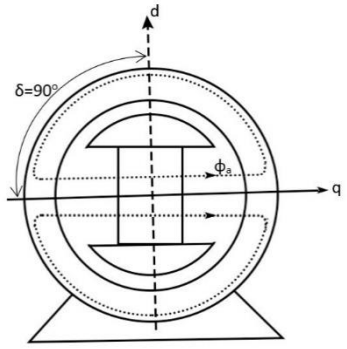

Fig. 8. Armature reaction magnetic flux $\emptyset_a$ of synchronous machine with salient pole directed along $q-axis$

Torque developed due to reluctance structure of the salient pole synchronous motor can be expressed as [22-23]:

$$T_r = \frac{3m}{2\omega} \frac{V_{ph}^2}{2} \left(\frac{1}{X_q} - \frac{1}{X_d} \right) \sin(2\delta) \quad (12)$$

But in case of excited or permanent magnet based salient pole synchronous motor the total torque is the summation of electromagnetic torque and reluctance torque which can be expressed as [23]:

$$T_s = \frac{3pE_aV_a}{2\omega X_d} \sin\delta + \frac{3p}{4\omega} \frac{V_{ph}^2}{2} \left(\frac{1}{X_q} - \frac{1}{X_d} \right) \sin(2\delta) = T_{em} + T_r \quad (13)$$

Where,

$p =$ number of poles

$\omega =$ synchronous angular velocity

$E_a =$ no load back EMF generated by the PMs

$X_d =$ direct reactance at the synchronous frequency

$X_q =$ quadrature reactance at the synchronous frequency

$T_s =$ synchronous torque

$V_a =$ input voltage

$\delta =$ torque angle

The torque versus power angle characteristics of the excited or permanent magnet based salient pole synchronous motor for a constant voltage is shown in the following diagram.

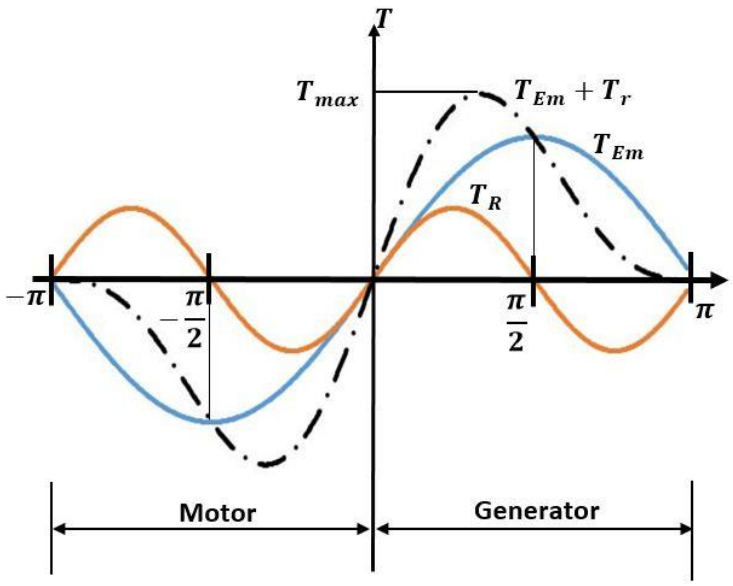

Fig. 9. Torque- power angle characteristics of synchronous machine with salient-pole rotor

2.6 Starting of synchronous motor

Synchronous motors are not inherently self-starting [16-17] [23]. As the stator magnetic field rotates at the synchronous speed as soon as the stator winding is supplied with three phase voltage supply, the rotor magnetic poles due to its inertia cannot latch with the poles of stator magnetic field and hence synchronous motor cannot start [16-17] [23]. There are different methods for the starting of the synchronous motors. The methods are briefly explained in the following section.

2.6.1 Start using variable-frequency drive

A synchronous motor can be started from low frequency using variable frequency drive and the frequency of the supply can be slowly ramped up to the corresponding operating frequency [21-22]. This method needs power electronic drive system. As the synchronous motor being dealt in this thesis is line start i.e. directly connected to the three phase supply from utility, starting of motor suing variable frequency drive is not applicable.

2.6.2 Self-starting with squirrel cage

A synchronous motor can also be started as an induction motor by embedding a squirrel cage on its rotor [21-22]. When the three phase field winding of a synchronous motor is supplied by AC current a rotating magnetic field is generated on the stator. There is a relative motion between the field and the rotor which induces an electric current on the conductive bars of the squirrel cage. The current flowing lengthwise on these squirrel cage bars react with the magnetic field of the rotor to create a tangential orthogonal force to the rotor, resulting on the torque responsible to turn the rotor shaft. When the rotor is turning at the same speed as the stator's rotating magnetic field, there is no relative speed between the squirrel-cage bars and the magnetic field of the stator hence no current is induced on the cage bars. At the synchronous speed the squirrel cage bars have no further effect on the steady state operation of the synchronous motor.

Chapter 3

LSPM Synchronous Motor Modelling in FEM

In order to analyze the LSPM synchronous motors Finite Element Analysis (FEA) method is applied using ANSYS Maxwell software. The simulations were performed in 3D Finite Element Mentoh (FEM). The software used for simulation and modelling is Ansoft ANSYS Maxwell. Maxwell is a powerful program that uses FEM to simulate finite distribution of mass. In this process a three-dimensional object is divided in small fundamental elements and then the differential equations which relates to electromagnetic phenomenon are solved at vertices of each of the fundamental elements. This process can be generalized in context of electromagnetic system as solving the set of Maxwell's equations. While solving the Maxwell equations initial condition and boundary for each of the fundamental elements are considered. Upcoming sections will bring light to the Maxwell's equations that are fundamental to understand how motors can be simulated using FEM.

3.1 Overview of Maxwell's equation

Mathematical formulations put forward by James Clark Maxwell about physical characteristics of electric and magnetic field serves as the base for the modern electromagnetics. These postulates helped define the main principle of electromagnetics and through Maxwell's equation the electromechanical conversion process is comprehended. Maxwell's equations can be fundamentally defined by the help of four fundamental equations:

3.1.1 Ampere's law

Ampere's law states the relation between the $electric\ current$ (I_c) and the $magnetic\ field$ $(\vec{H})$ as:

$$\oint_L \vec{H}\, d\vec{L} = I_C \tag{14}$$

Maxwell's study proposed a new type of current called $displacement\ current\ I_D$ which was incorporated with the equation (15) [24]. The $displacement\ current\ I_D$ is associated with the propagation of the above mentioned parameters in non-conductive materials. The propagation is expressed as flux of $displacement\ current\ density\ (\overrightarrow{J_D})$ for a specified cross section area. The relation between $\overrightarrow{J_D}$ and $electric\ flux\ density\ (\vec{D})$ can be expressed as [24]:

$$\overrightarrow{J_D} = \frac{\partial \vec{D}}{\partial t} = \varepsilon . \frac{\partial \vec{E}}{\partial t} \tag{15}$$

Maxwell added I_D in the scope of equation (14) to make the equation physically more consistent and expressed it as [31]:

$$\oint_L \vec{H}\, d\vec{L} = I_C + I_D \tag{16}$$

Equation (16) can also be expressed as equation (17) by expressing currents in terms of flux of current densities $(\vec{J})$.

$$\oint_L \vec{H}\, d\vec{L} = \oiint_s \overrightarrow{J_C} d\vec{S} + \oiint_s \overrightarrow{J_D} d\vec{S} \tag{17}$$

or $$\oint_L \vec{H}\, d\vec{L} = \oiint_s (\overrightarrow{J_C} + \overrightarrow{J_D}) d\vec{S} \tag{18}$$

After aplying Stokes theorem to equation 19, it can be rewritten as:

$$\vec{\nabla} x \vec{H} = \overrightarrow{J_C} + \overrightarrow{J_D} \tag{19}$$

Equation 18 is also known as the Maxwell's first equation in differential form and it describes the rotational nature of $magnetic\ field\ (\vec{H})$ [24].

3.1.2 Faraday's Law

Faraday's law states that the $voltage\ induced$ (V_{IND}) in a conductor is due to the temporal variation of $magnetic\ flux$ (ϕ_m) around the conductor [24]. It is expresses as:

$$V_{IND} = -N\left(\frac{d\phi_m}{dt}\right) \tag{20}$$

Expressing V_{IND} in terms of $electric\ field$ $(\vec{E})$ and ϕ_m in terms of $magnetic\ flux\ density$ $(\vec{B})$:

$$\int_L \vec{E}d\vec{L} = -N.\iint_s \frac{\partial \vec{B}}{\partial t}\, d\vec{S} \tag{21}$$

Equation 21 is called Maxwell's second equation and by applying Stoke's law can be expressed as:

$$\int_L (\vec{\nabla} x \vec{E}) d\vec{S} = \iint_s \left(-N.\frac{\partial \vec{B}}{\partial t}\right) d\vec{S} \tag{22}$$

$$\vec{\nabla} x \vec{E} = -N.\frac{\partial \vec{B}}{\partial t} \tag{23}$$

3.1.3 Gauss' Law applied to magnetism

Gauss' law states that the net magnetic flux out of any closed surface is zero. It also describes the in existence of single magnetic pole [24]. Gauss' lay can be expressed as:

$$\oiint_S \vec{B}d\vec{S} = \vec{0} \tag{24}$$

Which is the Maxwell's third equation in integral form. By applying divergence theorem (Gauss' Theorem) equation (24) can also be expressed as:

$$\iiint \vec{\nabla}.\vec{B}\, d\vec{V} = 0 \tag{25}$$

or $$\vec{\nabla}.\vec{B} = \vec{0} \tag{26}$$

3.1.4 Gauss' Law

Gauss Law states that the electric flux around a closed surface is equivalent to the total $chanrge\ (Q_T)$ inside the geometry represented as:

$$\oiint_S \vec{D} d\vec{S} = Q_T \tag{27}$$

As charge can also be represented by the $volumetric\ density\ (\rho_v)$ the Maxwell's fourth equation can be written in the integral form as [24]:

$$\oiint_S \vec{D} d\vec{S} = \iiint_V \rho_v \, dV \tag{28}$$

or $$\oiint_S \varepsilon . \vec{E} d\vec{S} = \iiint_V \rho_v \, dV \tag{29}$$

or $$\oiint_S \vec{E} d\vec{S} = \iiint_V \frac{\rho_v}{\varepsilon} \, dV \tag{30}$$

Now using divergence theorem equation (30) can further be expressed as:

$$\oiiint_V \nabla . \vec{E} d\vec{S} = \iiint_V \frac{\rho_v}{\varepsilon} \, dV \tag{31}$$

or $$\nabla . \vec{E} = \frac{\rho_v}{\varepsilon} \tag{32}$$

3.2 Modelling by Maxwell V16 Program

Maxwell is an interactive software package that uses finite element analysis (FEA) to solve three dimensional (3D) electrostatic, magnetostatic, eddy current, and transient problems. Using Maxwell following things can be done:

- Static electric fields, forces, torques, and capacitances caused by voltage distributions and charges.

- Static magnetic fields, forces, torques, and inductances caused by DC currents, static external
- magnetic fields, and permanent magnets.
- Time-varying magnetic fields, forces, torques, and impedances caused by AC currents and
- oscillating external magnetic fields.
- Transient magnetic fields caused by electrical sources and permanent magnets.

RMxprt™ is an interactive software package used for designing and analyzing electrical machines. Maxwell and Rmxprt are integrated into the ANSYS Electronics Desktop.

3.2.1 Maxwell Desktop

Fig. 10. presents the screenshot of the Maxwell V16 desktop when the software is launched. The picture shows different parts which are used while modelling in Maxwell.

- **Menu Bar**: Menu bar is used to perform various tasks ranging from creating new projects, opening project, editing, drawing objects to setting and modifying project parameters.
- **Tool bar**: The toolbar buttons and shortcut pull-down lists act as shortcuts for executing various commands. To execute a command, toolbar button or a selection is clicked on the shortcut pull-down list.
- **Project Manager**: Project manager contains the project structure of the project that is running in the Maxwell. Project manager has a tree structure and project title follows the excitation, boundaries, analysis and results.

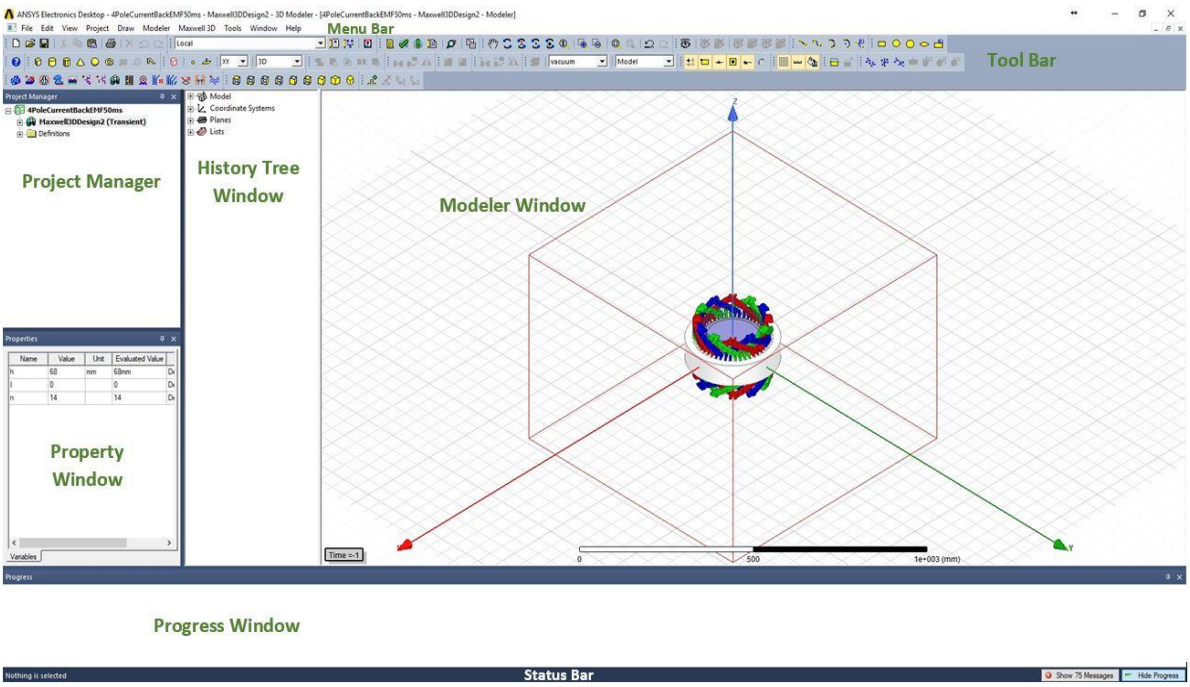

Fig. 10. Maxwell desktop window

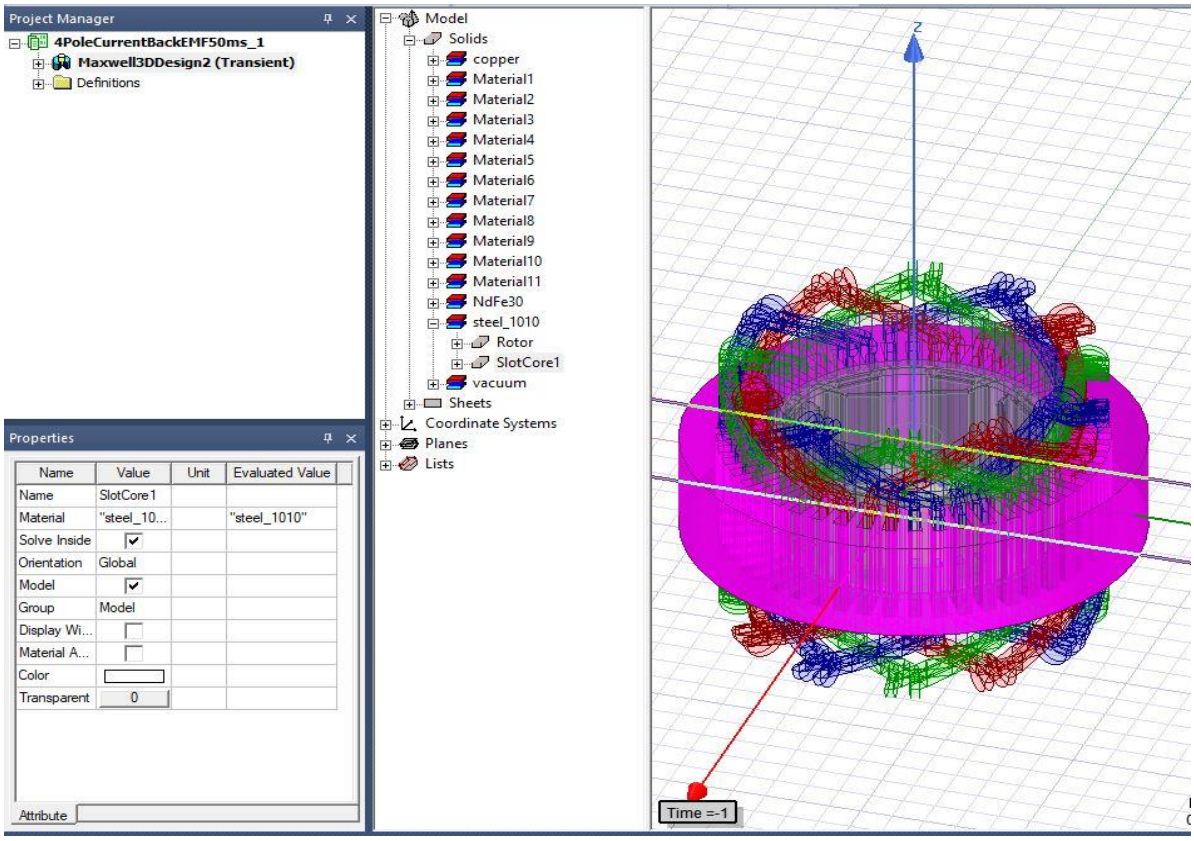

Fig. 11. Property Window

- **Property window**: Property window (Fig. 11.) displays the properties of the materials that is selected in the project tree or in the Maxwell 3D modeler window. From the property window we can assign or edit the properties of any selected components.
- **3D Modeler window**: Modeler window is the workspace where any design is created. The modeler window has axes marked with x-, y- and z- axis by default.

3.2.2 Drawing Tools

Maxwell V16 can be used to draw 1D, 2D and 3D electromagnetic model. The set of tools used to models objects in the modeler are listed under Drawing Tools. Drawing tools can be One-Dimensional, Two-Dimensional or Three-Dimensional. But to use these tools the first task is to open a new project. Default name for the new project is "project1" and is displayed in project manager window. The project file is double clicked in the project tree to open. There are different drawing tools available in Toolbar.

- **One-Dimensional (1D):** 1D objects in general are called polylines which includes straight lines, arc lines or spline segment. Such polylines can be accessed by clicking the icons in Toolbar as shown in Fig. 12.

Fig. 12. 1D Tools

- **Two-Dimensional (2D):** 2D objects are the closed boundary objects which includes, rectangles, circles etc. The tool bar shown in Fig. 13 can be used to access the 2D polygons.

Fig. 13. 2D Tools

- **Three-Dimensional (3d):** 3d Objects include cuboid, cylinder, sphere, cones etc. The 3D objects can be drawn by accessing the icons as shown in Fig. 14 from Tool bar. Maxwell also has a feature to convert 2D object to 3D object by thickening the 2D objects as shown in Fig. 15.

Fig. 14. 3D Tools

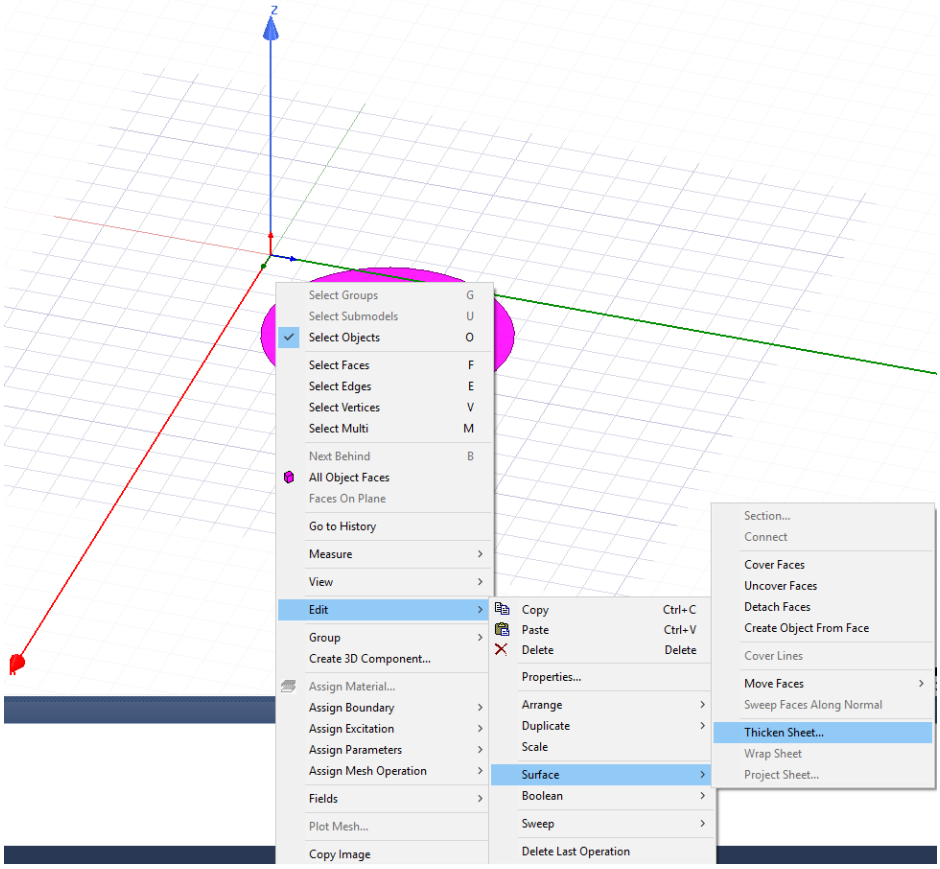

Fig. 15. Thickening 2D sheet objects into 3D objects

In order to draw an object, “Draw” on menu bar can selected and particular object such as box, sphere, cylinder etc. can be drawn. Alternatively, the shortcut can be selected in the Toolbar. For example, if a box is to be drawn, first the box tool is selected and a box is drawn in the modeler space or X-, Y- and Z-starting points can be entered followed by the specified dX, dY and dZ to define dimensions in each axes.

There are other tools which are common during the design process which includes Boolean operations such as splitting, uniting, subtracting etc., duplicating options such along line, along axis etc. Fig. 16 shows the available Boolean Edit tools.

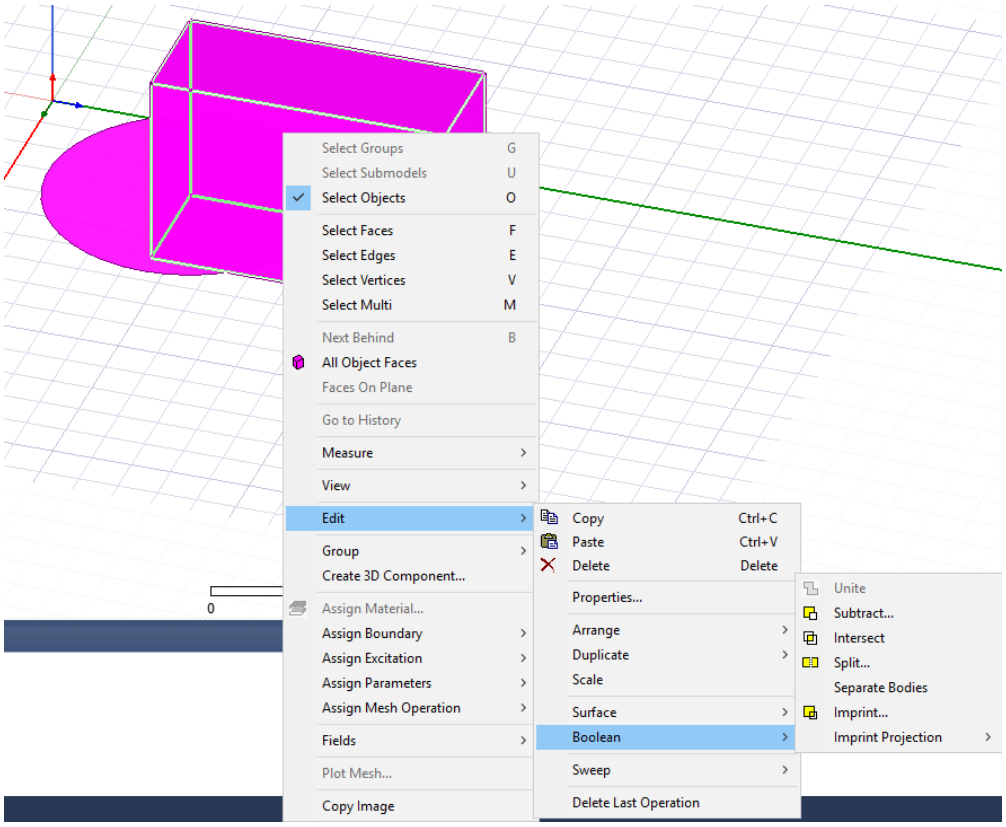

Fig. 16. Boolean edit tools

3.2.3 Preprocessor Mode

After designing the simulation model one of the most important task to be done is material assignment. Maxwell has many materials available in its library which can be assigned as per user's choice. To assigns material first the component in the model is selected. Then "Modeler" needs to be clicked from menu bar followed by "Assign Material". The following window as shown in Fig. 17 is seen. Alternatively, In the property window the material value can be edited to get the window as shown in Fig. 17.

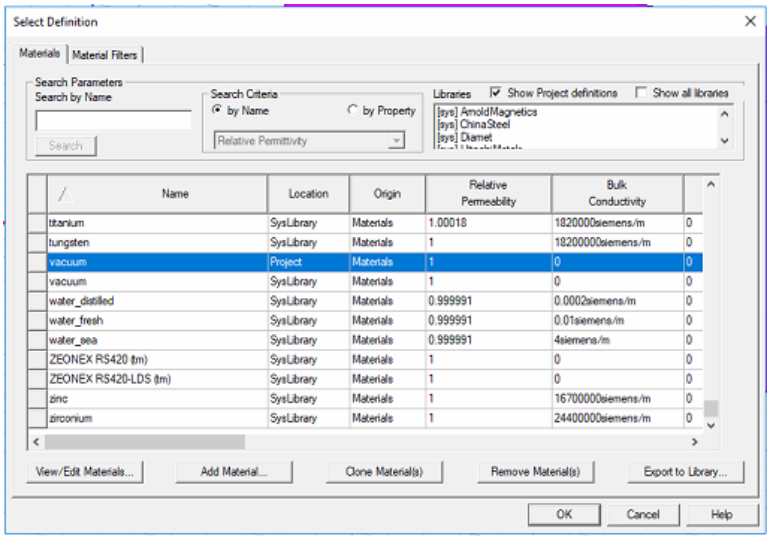

Fig. 17. Material Assignment Window

3.2.4 Motion Modelling in Maxwell

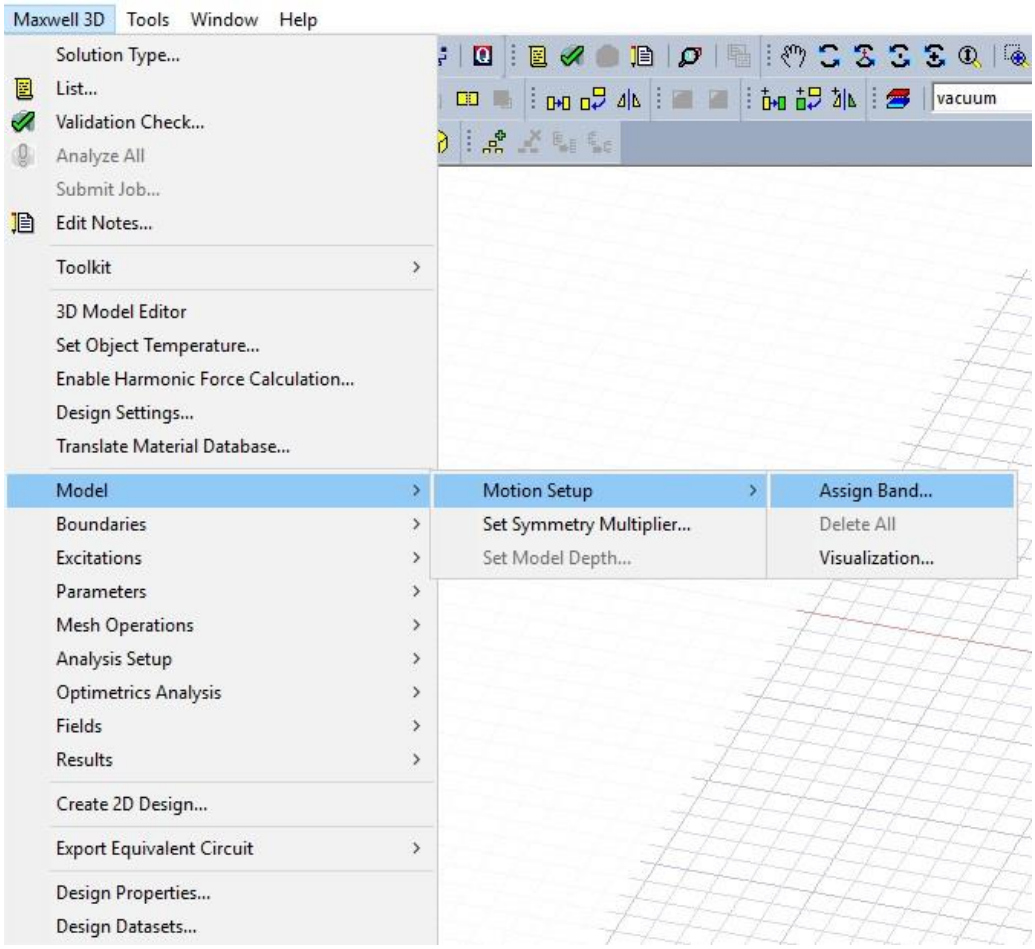

Fig. 18. Assigning Band Object for Motion Modelling

In order to model motion in the Rotor Structure the rotor must be isolated from rest of the model using a mesh band. Usually two mesh bands inner and outer are used for motion modelling. Mesh band are regular polyhedron with finite number of segments whose material is assigned as Vacuum (which should be the default). Again another cylinder should be constructed smaller in diameter than the polyhedron for the band enclosing the rotor completely. Then to assign the motion to the mesh band, mesh band is selected then **Assign Band** is clicked on **Maxwell3D>Model>Motion Setup** as seen in Fig. 18. Then Motion Type is selected as Rotational (since transitional motion simulation is also possible), Rotational axes is selected followed by entering the mechanical transients such as moment of inertia and damping if data is available.

3.2.5 Set Up the Transient Analysis

To set up a Transient analysis:

1. Right-click **Analysis** in the project tree.

   A shortcut menu appears.

2. Select **Add Solution Setup**.

   The **Solve Setup** dialog box appears.

3. Click the **General** tab.
4. Type **0.9** in the **Stop time** box, and select **s** as the unit.
5. Type **0.005** in the **Time step** box, and select **s** as the unit.
6. Add a sweep:
   a. Click the **Save Fields** tab.
   b. Select **Linear Step** from the **Type** pull-down list to identify the type of sweep.
   c. Type **0.0** in the **Start** box.
   d. Type **Simulation end time** in the **Stop** box.

e. Type **step size** in the **Step Size** box.

f. Click **Add to List**.

7. Click **OK**.

To run the transient analysis under the Analysis tab in the project tree Transient setup should be right clicked followed by clicking Analyze.

Chapter 4

Two-Speed LSPM Synchronous Motor

4.1 Scheme I: Reluctance Structure Overlaid on Permanent Magnet

4.1.1 Principle of Operation

The LSPM Synchronous Motor design is based on variable pole numbers for the stator and the rotor. The LSPMSM is also capable of operating in two different speeds without requiring a drive unit. PMs are specially arranged so that the rotor contains a 4-pole PM configuration overlaid on an 8-pole reluctance configuration. For the stator to act as 4-pole or 8-pole structure there are two possible pole changing configuration; Dahlander type winding and multiple independent windings with different number of poles. In this design the second approach is used and the stator is reconfigured by two separate windings to change the operating pole count is used.

Stator windings present are of two different pole number (4/8) and these windings are switched in order to change the pole count for low speed and high speed operations. Two different types of windings are presented in Fig. 19. For the motor to be able to rotate in two different speeds, the rotor must also be designed such a way that it can adapt to the change in pole number of stator. To achieve this rotor is designed in such a way that it has one magnetic polarity from the nature of permanent magnet present and another magnetic polarity from the reluctance nature of the rotor core. Equation (33) shows that the produced synchronous consists of two terms; permanent magnet torque and reluctance torque.

$$T_s = \frac{3p}{2\omega_s}.\frac{E_o U}{X_{ds}}\sin(\delta) + \frac{3p}{4\omega_s}.\frac{U^2(X_{ds}-X_{qs})}{X_{ds}.X_{qs}}sin(2\delta) \quad (33)$$

Where,

$p =$ number of poles

ω_s = synchronous angular velocity

E_o = no load back EMF generated by the PMs

X_{ds} = direct reactance at the synchronous frequency

X_{qs} = quadrature reactance at the synchronous frequency

T_s = synchronous torque

U = input voltage

δ = torque angle

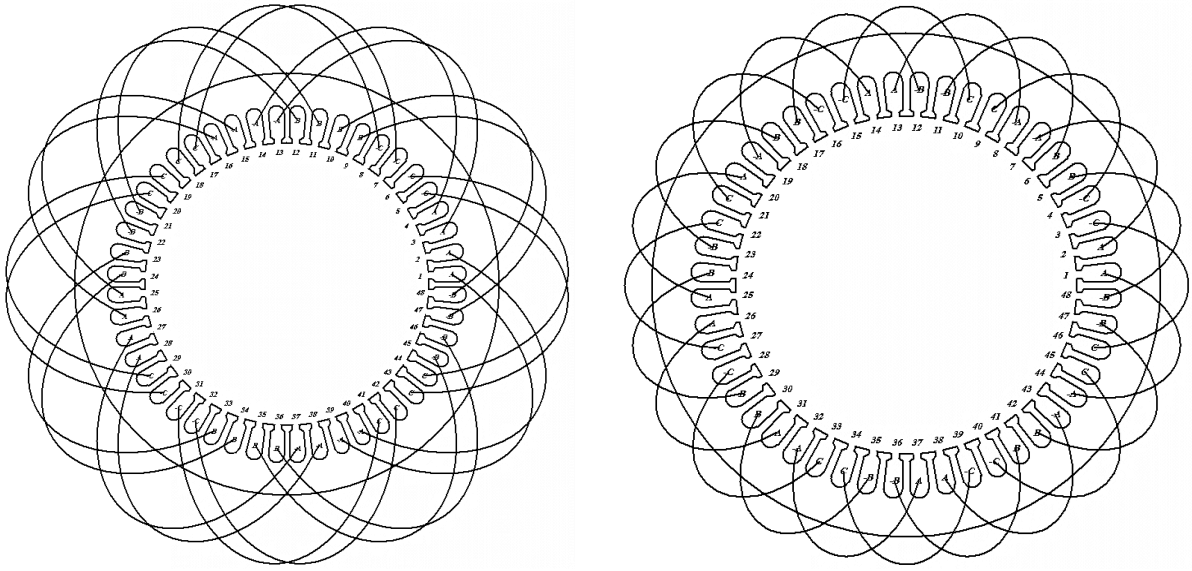

(a) (b)

Fig. 19. The stator winding arrangement (a) 4-pole, (b) 8-pole.

For the analysis of this motor, if the nature of the rotor pole from stator pole's perspective is seen, the magnetic properties of the permanent magnets are neutralized at low speed region and the permanent magnet nature doesn't affect the motor performance. Which also means the reluctance nature of the motor is dominant at the low speed region. Whereas, in case of high speed the reluctance nature is neutralized and magnetic property is dominant. It is substantial to note that

this methodology is general and can be extended to any number of arbitrary pole.

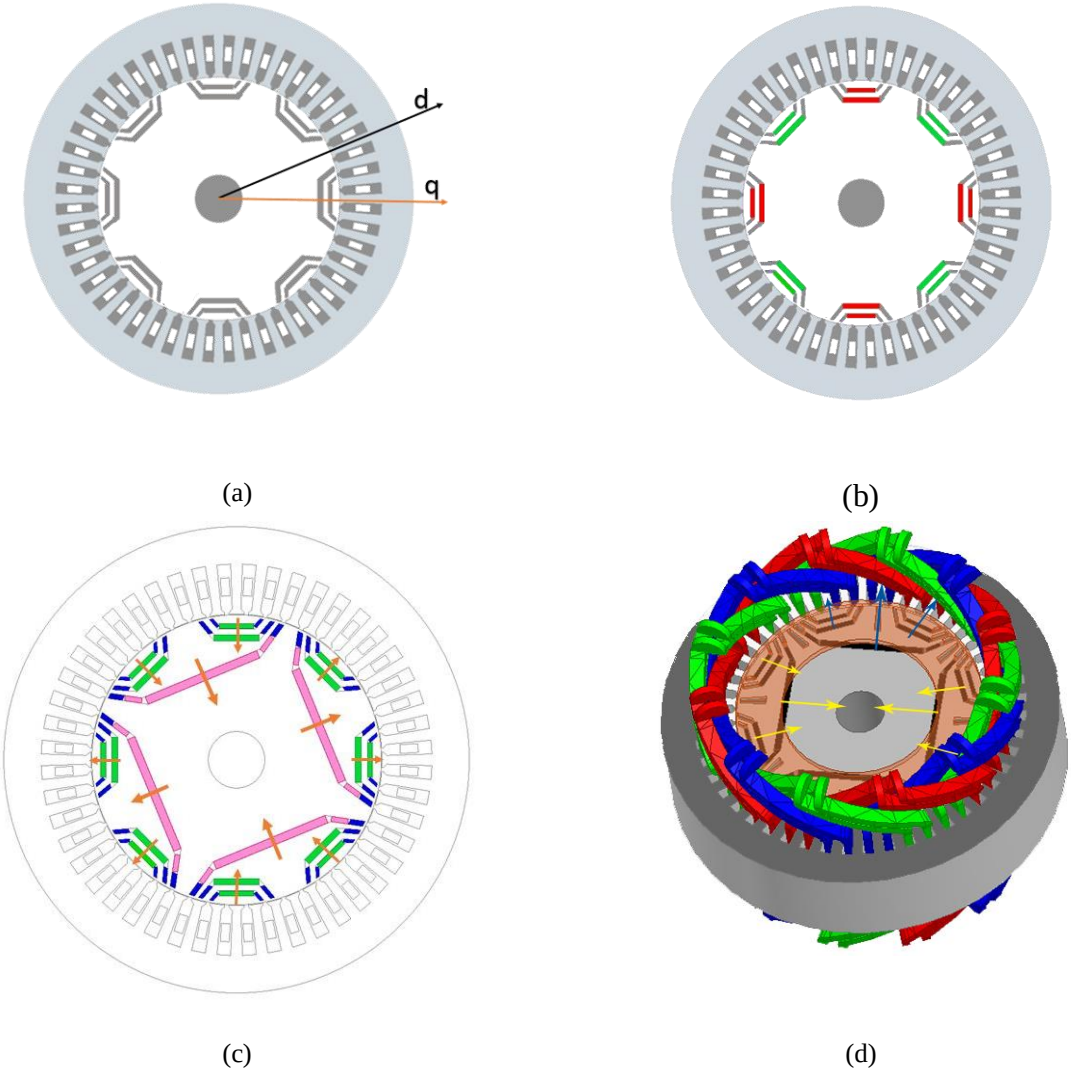

Fig. 20. Schematic of the motor (a) 8-pole reluctancec structure (b) 8-pole reluctancec structure with permanent magnet assist(c) 2-D of Designed 4/8-pole motor (d)3-D of designed 4/8-pole motor

Fig. 20(c) depicts the schematic of the proposed motor with 4/8 pole structure to operate at 1500/750 rpm. This design is similar to 8-pole reluctance motor as shown in Fig. 20(a) with the PMs added to the rotor as shown in Fig. 20(b). This rotor arrangement works in such a way that the magnets create four-pole permanent magnet structure and the slots creates the eight-pole reluctance structure. It can also be seen in Fig. 20(c) that four supplementary permanent magnets are implanted in the rotor in order to increase the permanent magnet torque, increase the flux

through the middle of each pole (i.e., alternately between adjacent reluctance poles) and decrease the harmonics of the induced back-EMF.

Even though additional PMs reduces the reluctance difference between the d and q-axis which lowers the reluctance torque, it does not negatively impact the motor operation as the motor is designed for a fan-type load in which the torque is proportional to the square of the rotor speed and the required torque for the eight-pole run (reluctance torque) is one fourth of that for the four-pole run (PM torque).

Fig. 21 and Fig. 22 shows magnetic flux lines and distribution of flux density at no load respectively. These result help deduce that the motor is not saturated.

The interaction between the induced back-EMF and the stator current causes the braking torque equation (34) opposing the electromagnetic torque which may cause a failing in starting or synchronization of the motor. To address this issue, the rotor cage bars are located at the end of flux barriers as deep as possible [7].

$$T_b = \frac{3p}{2\omega_s} . E_o^2 R_1 (1-s) \frac{R_1^2 + (1-s)^2 X_{qs}^2}{\left(R^2 + (1-s)^2 X_{ds} X_{qs}\right)^2} \quad (34)$$

Where,

$T_b =$ braking torque

$R_1 =$ stator resistance

$s =$ motor slip

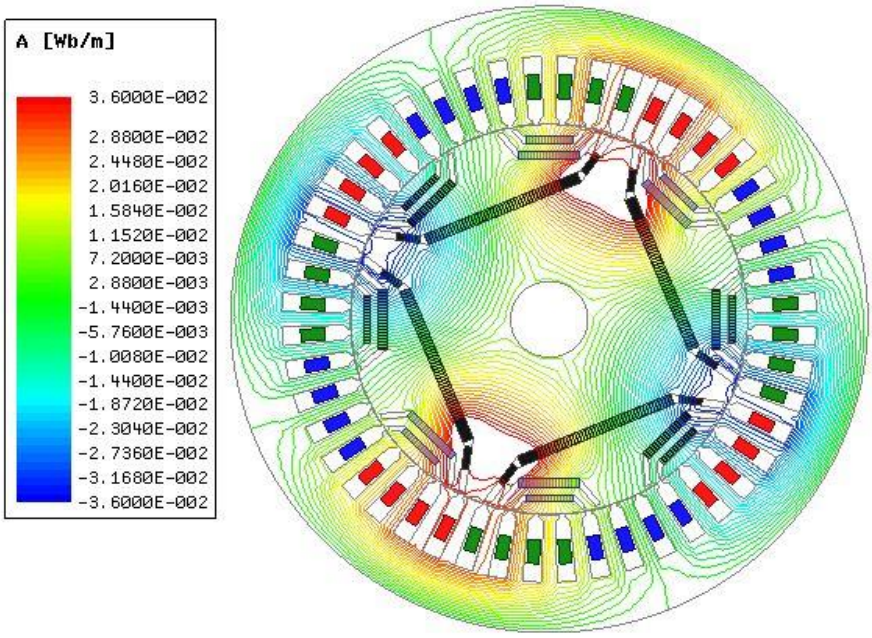

Fig. 21. Magnetic flux lines at no load.

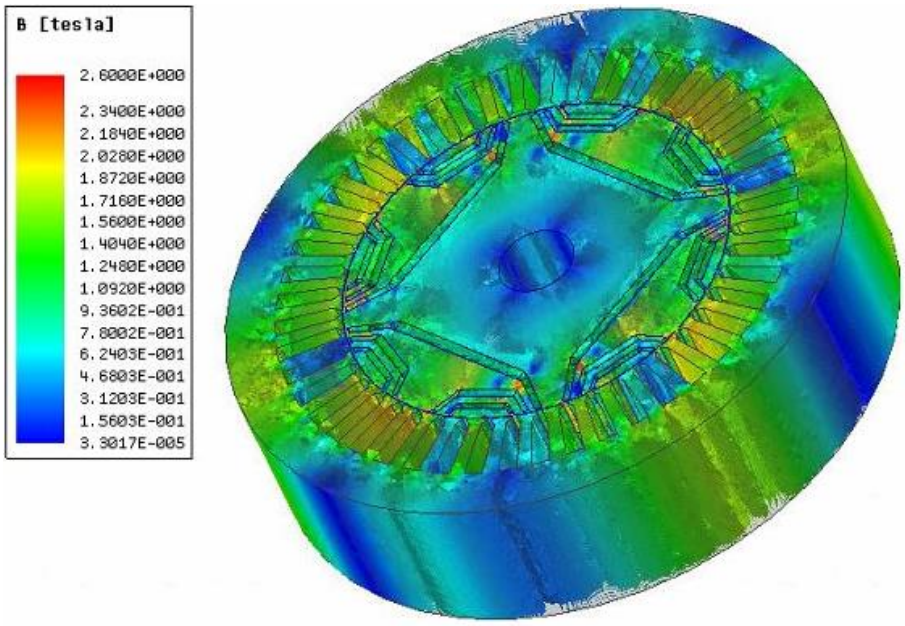

Fig. 22. Distribution of flux density at no load.

4.1.2 Modelling of LSPM: Scheme I

Design parameters for the LSPMSM is shown in Table 1. The design data for different components will be discussed in the following sections.

TABLE I. DESIGN DATA OF THE TWO-SPEED MOTOR: SCHEME ONE

Stator	**Outer diameter**	284 mm
	Inner diameter	175 mm
	Stack length	68 mm
	Number of slots	48
	Conductor per slot for high	34
	Conductor per slot for low	52
Rotor	**Outer diameter**	174.2 mm
	Inner diameter	34 mm
	Inertia	0.04 kgm^2
	B_r of magnets	1.1 tesla
Load	**Inertia**	0.02 kgm^2

4.1.2.1 Stator

The stator of LSPMSM was designed in ANSYS Maxwell using RMxprt tool. RMxprt is a template-based design tool. The design parameters for RMxprt design of stator is presented below in Table II. Fig. 23 shows the parameters used for design of stator slot. Fig 24 shows the designed stator.

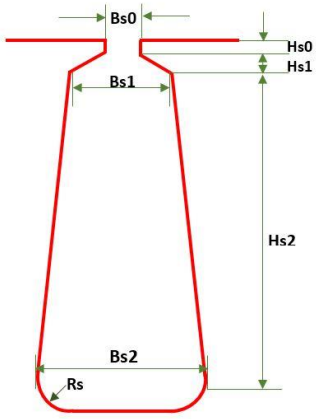

Fig. 23. Stator slot design parameter

TABLE II. DESIGN PARAMETERS FOR STATOR

S.No.	Parameter Name	Value	Unit
1	Dia Gap	175	mm
2	Dia Yoke	280	mm
3	Length	68	mm
4	Skew	0	deg
5	Slots	48	
6	Slot Type	3	
7	Hs0	1	mm
8	Hs01	0	mm
9	Hs1	2	mm
10	Hs2	27	mm
11	Bs0	2.5	mm
12	Bs1	6.6	mm
13	Bs2	8.3	mm
14	Rs	0	mm
15	Fillet Type	0	
16	Half Slot	0	
17	Seg Angle	15	deg
18	Len Region	200	mm
19	Info Coil	0	

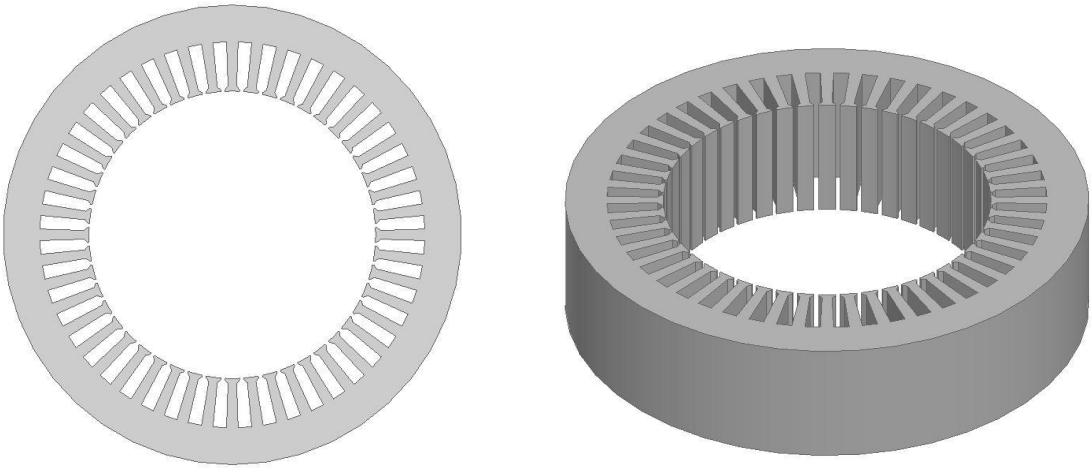

(a) (b)

Fig. 24. Stator (a) Top View (b) Isometric View

4.1.2.2 Rotor

The rotor design is as shown in Fig. 25. This rotor is custom designed for LSPM synchronous motor and accommodates the permanent magnet in the slot such that the magnets form four-pole permanent magnet structure and the slots create reluctance structure to form eight-pole. The rotor also consists of squirrel cage for self-starting.

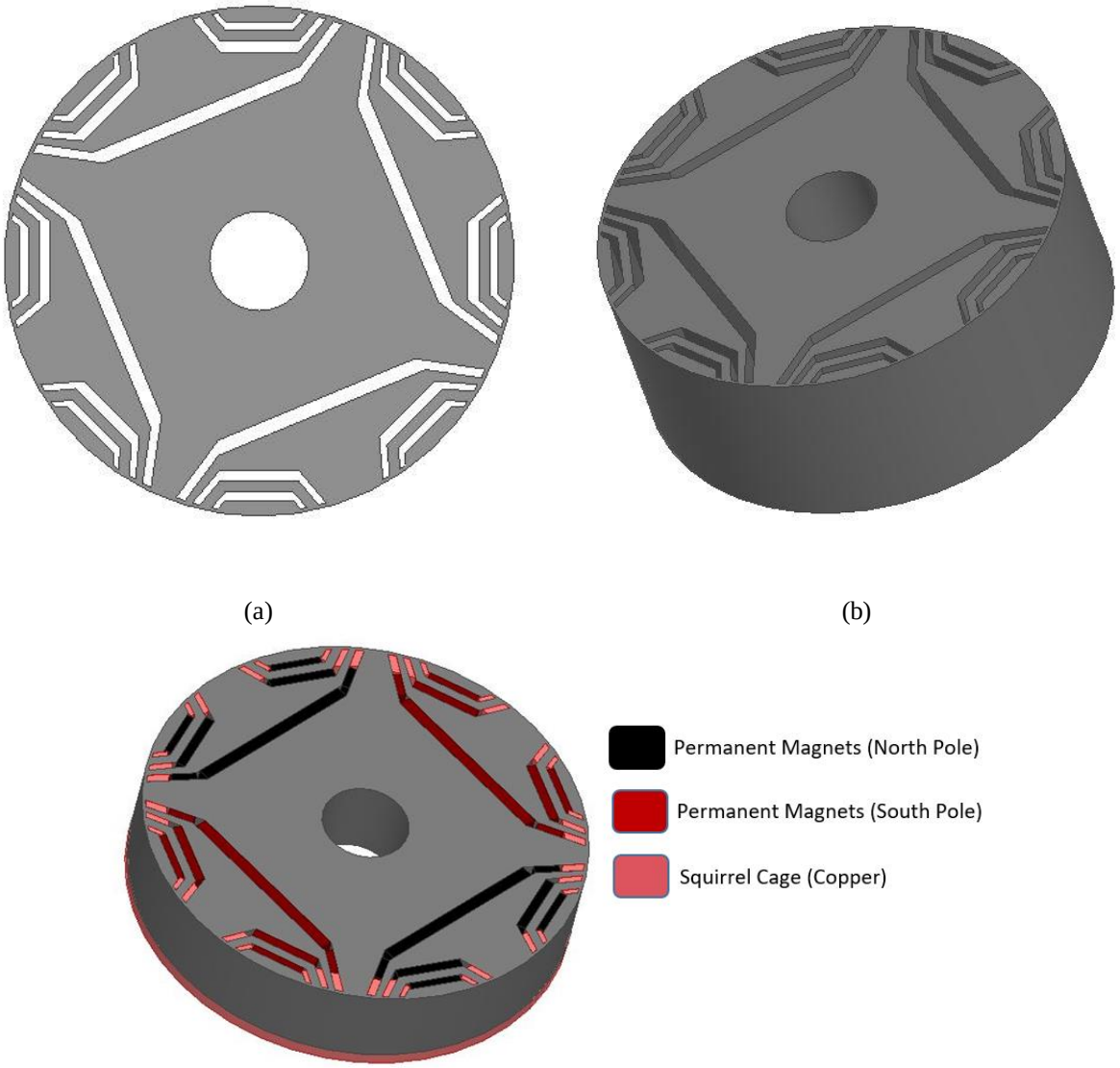

Fig. 25. Rotor Design (a) Top View (b) Isometric View (c) Half section view with permanent magnets and squirrel cage

4.1.2.3 Squirrel Cage

LSPMSM rotor has a squirrel cage embedded on it for self-starting. The squirrel cage is made up of copper bars shorted on both ends with copper ring as shown in Fig. 26. For the starting of synchronous motor, the cage bars must be as deeply embedded as possible [7] which is achieved by locating at the end of flux barriers of the rotors. Fig. 25 (c) shows the arrangement of squirrel cage inside the rotor.

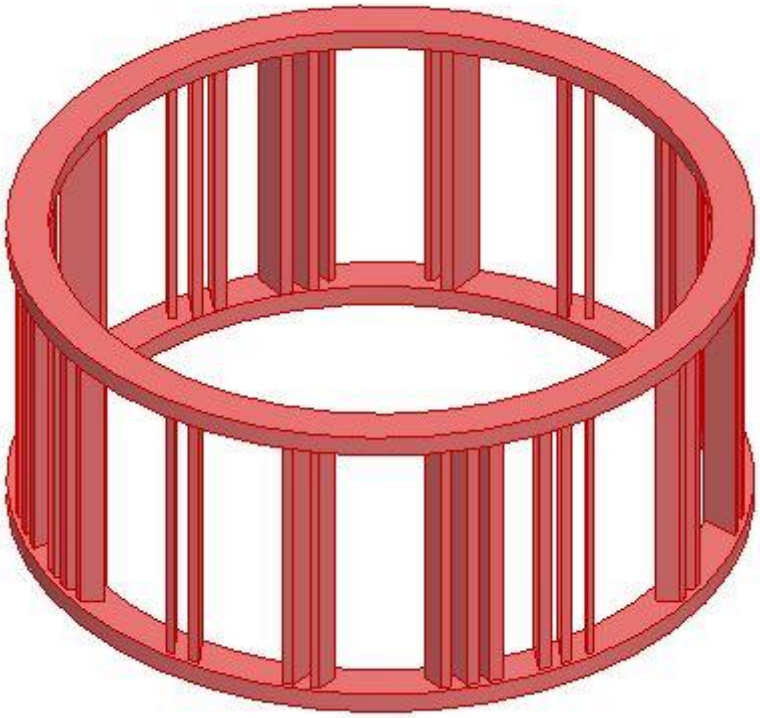

Fig. 26. Squirrel Cage bars

4.1.2.3 Windings

The four-pole as well as eight-pole winding of LSPMSM was also designed in ANSYS Maxwell using RMxprt tool. The design parameters for RMxprt design of both the winding is presented below in Table III. Fig 27 shows the designed windings. In Fig. 27 three phases are indicated by different color viz. green, red and blue. In actual LSPMSM both of these windings are presented in same stator and are separately excited as per the speed requirement.

TABLE III. DESIGN PARAMETERS FOR FOUR-POLE AND EIGHT-POLE WINDINGS

		4 Pole Coil	**8 Pole Coil**	
S.No.	**Parameter Name**	**Value**	**Value**	**Unit**
1	Dia Gap	175	175	mm
2	Dia Yoke	284	284	mm
3	Length	68	68	mm
4	Skew	0	0	deg
5	Slots	48	48	
6	Slot Type	3	3	
7	Hs0	1.5	1.5	mm
8	Hs1	4	4	mm
9	Hs2	5	20	mm
10	Bs0	5	5	
11	Bs1	8	8	mm
12	Bs2	8.5	8.5	mm
13	Rs	0	0	mm
14	Fillet Type	0	0	
15	Layers	1	1	
16	Coil Pitch	10	5	
17	End Ext	5	5	mm
18	Span Ext	25	25	mm
19	Bend Angle	0	0	deg
20	Seg Angle	10	10	deg
21	Len Region	200	200	mm
22	Info Coil	0	0	

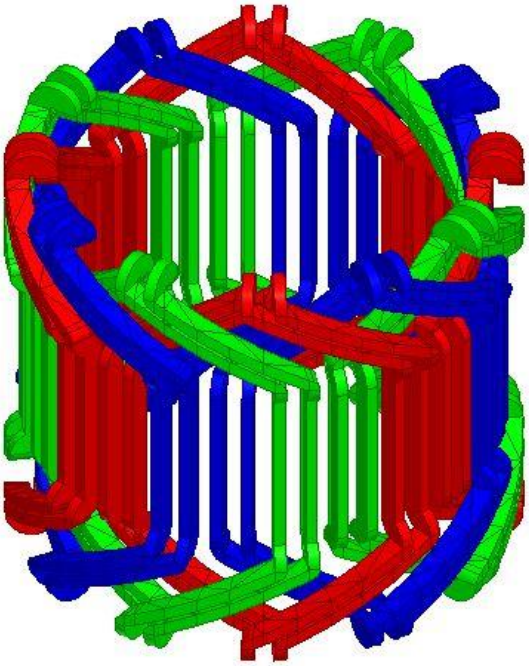

(a)

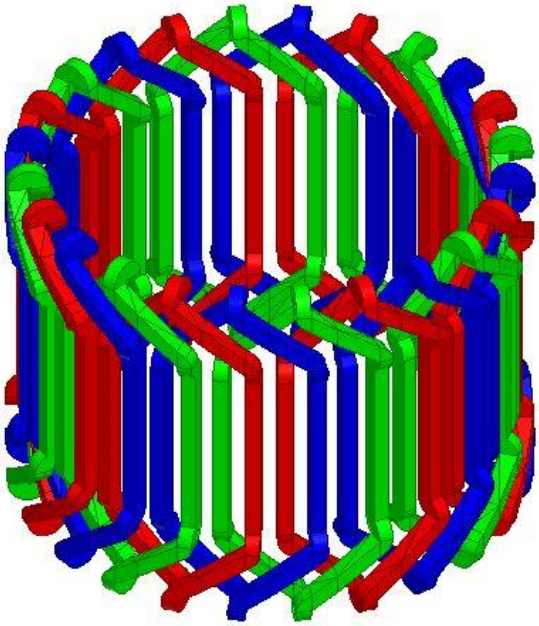

(b)

Fig. 27. Winding design (a) Four-Pole (b) Eight-Pole

4.1.3 Simulation and Results

4.1.3.1 Steady State Analysis

Induced Back EMF at synchronous speed (1500 rpm) for four-pole run is shown in Fig. 28. Plainly, it is evident that the four additional permanent magnets have strengthen the flux through the middle of each pole (i.e. between two adjacent poles) which has contributed to more sinusoidal waveform.

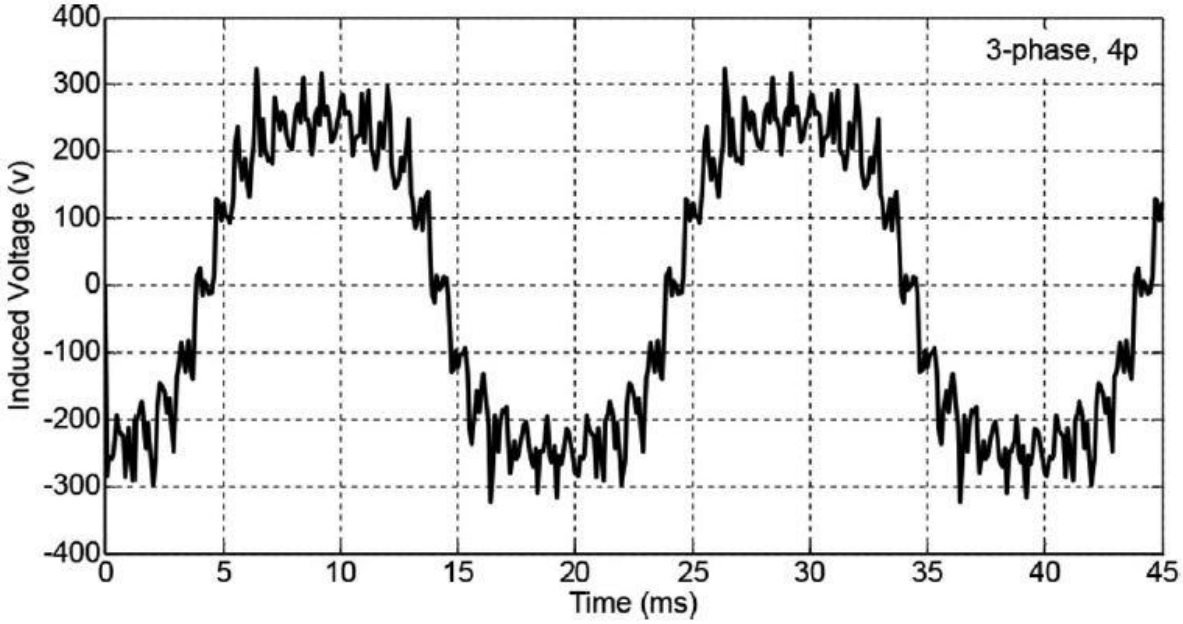

Fig. 28. Per phase back-EMF at synchronous speed (4-pole run).

Torque versus power angle characteristics at synchronous speed for four-pole and eight-pole run is shown in Fig. 29. It is evident from that the maximum torque generated during high speed (four-pole run) is about four times the maximum torque generated at low speed (eight-pole run) which is suitable for a fan type load. Also, it can be noticed that permanent magnet torque and reluctance torque is not completely eliminated for eight-pole and 4-pole run, which is responsible for non-purely sinusoidal torque profiles.

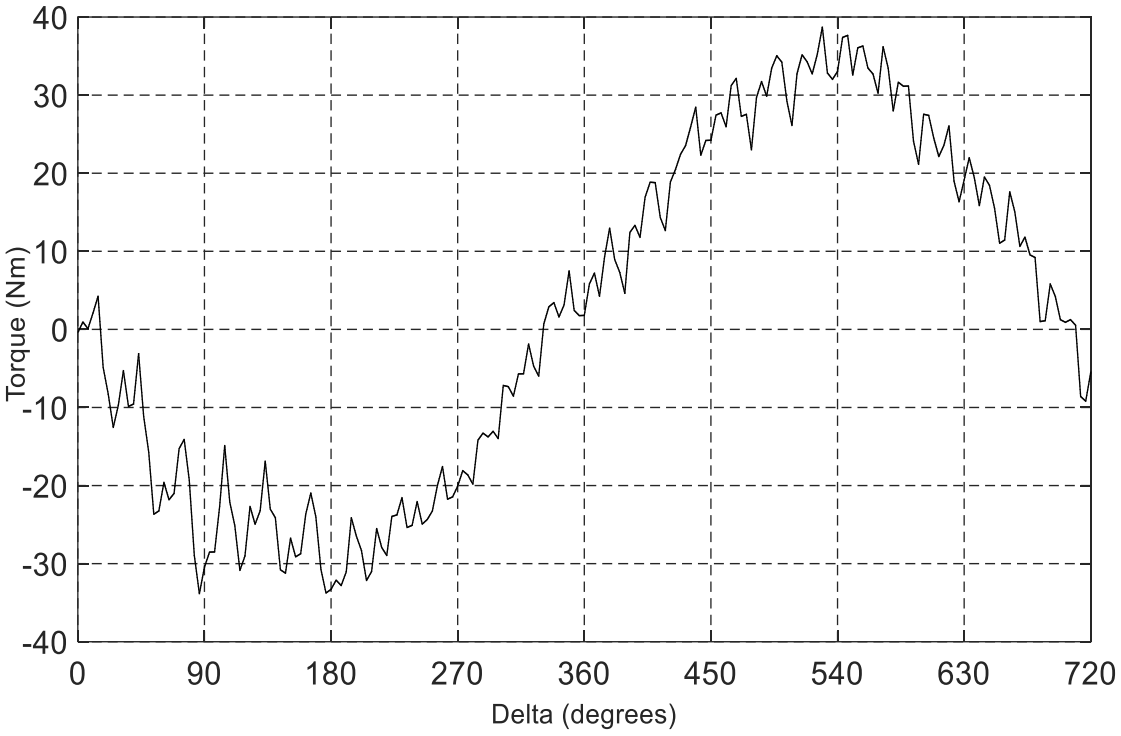

(a)

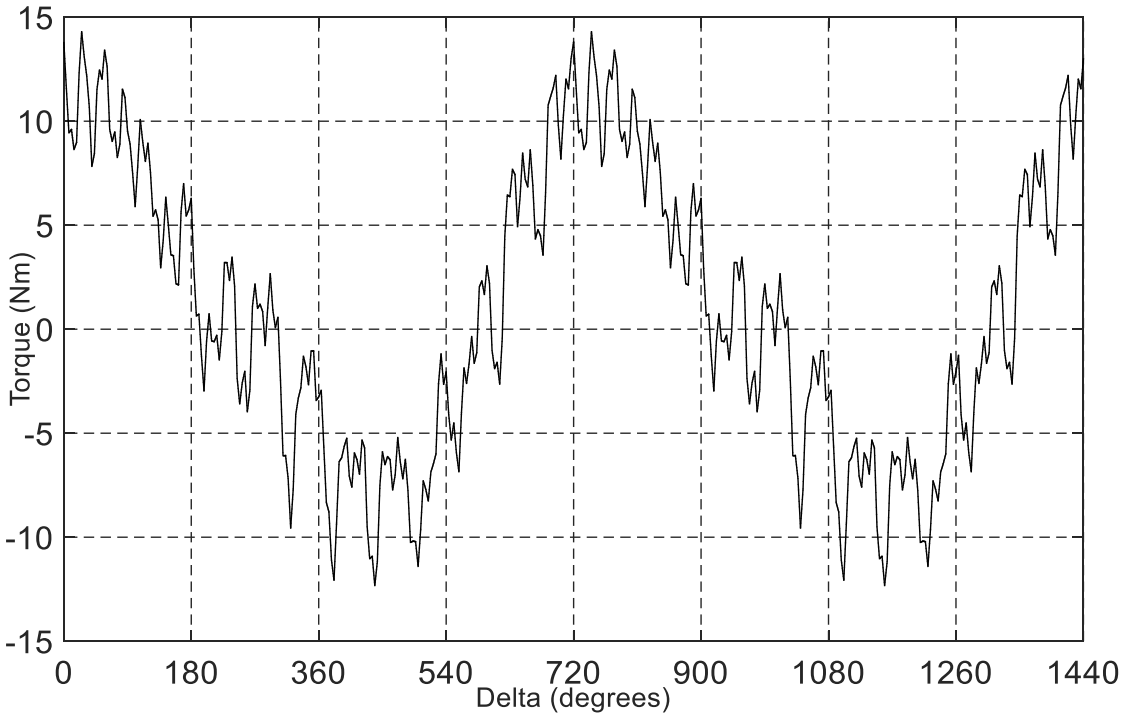

(b)

Fig. 29. Synchronous torque versus power angle a) 4-pole run, b) 8-pole run.

4.1.3.2 Transient Analysis

Load torque is proportional to square of speed for most application such as fans, compressors and pumps. Load torque equation is given by equation 35.

$$T_L = k\omega^2 \tag{35}$$

Fig. 30 shows the speed torque response as explained by Eqn. 34.

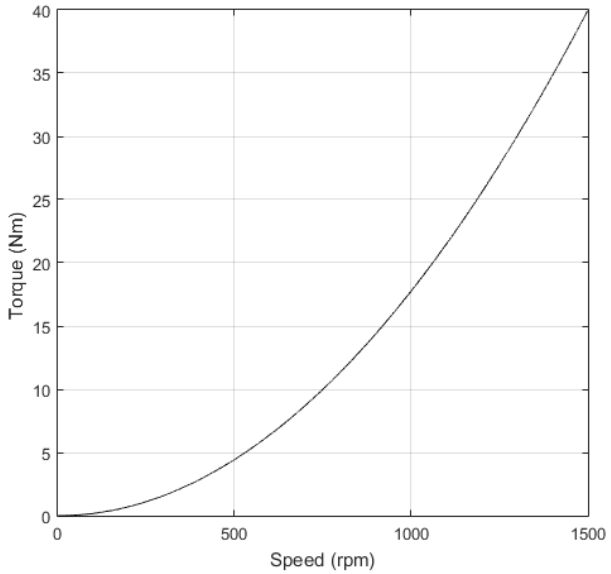

Fig. 30. Speed Vs. Torque Response

For the case study done for this thesis the load torque is 40Nm at the speed of 1500 rpm and 10 Nm at the speed of 750 rpm. 380 Volts line to line is applied in case of both four-pole and eight-pole stator winding. Fig. 31 shows the speed-time response of the motor starting for the 4-pole operating mode is depicted. The figure shows that the designed LSPMSM can start successfully and after the transient time it reaches the synchronous speed (≈ 1500 rpm).

Fig. 32 and Fig. 33 shows characteristics of torque and the stator phase current during the motor start. After some time, the torque and phase currents settle at their steady state value.

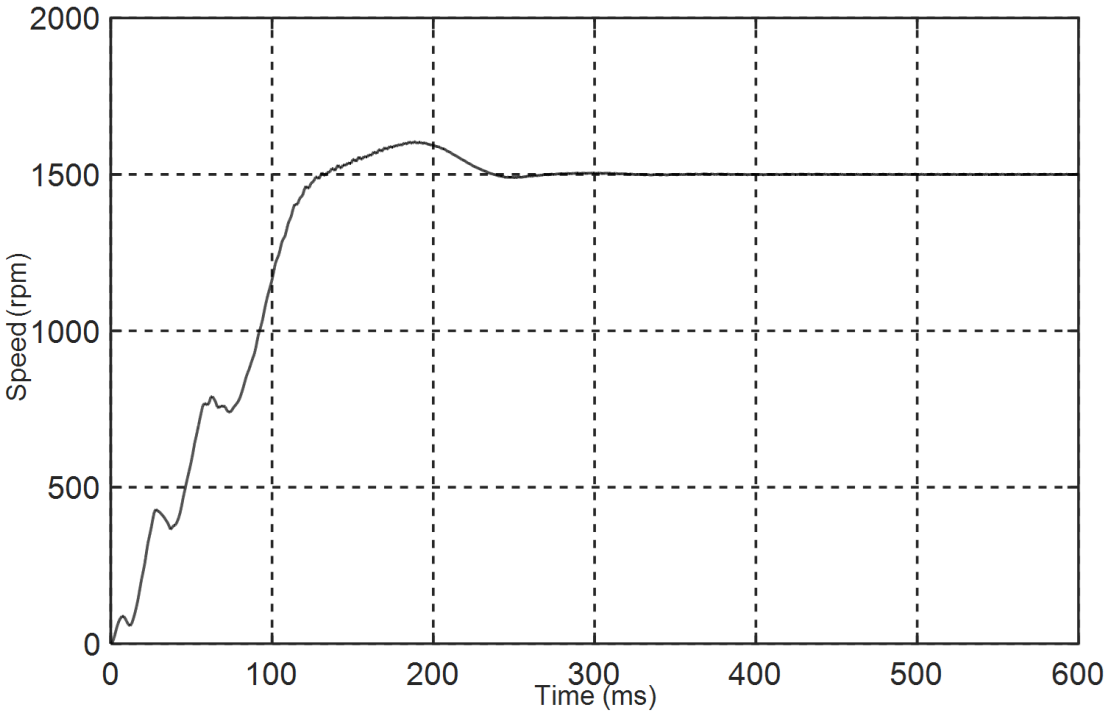

Fig. 31. Starting transient speed response of the motor in 4-pole run

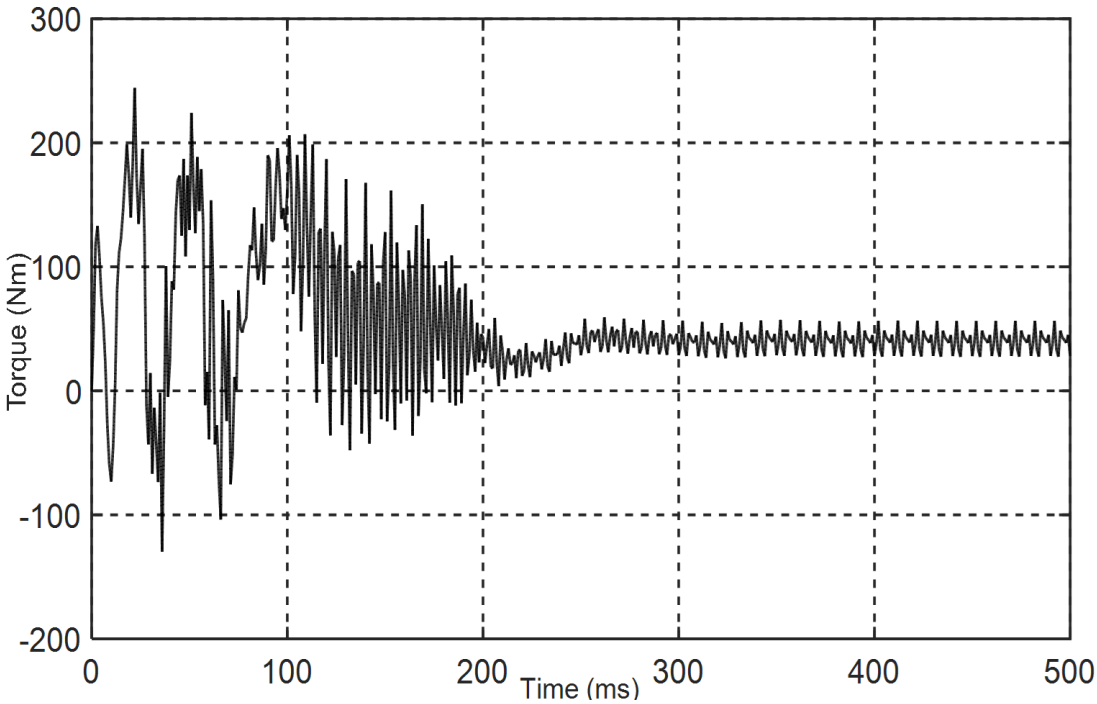

Fig. 32. Starting transient torque response of the motor in 4-pole run

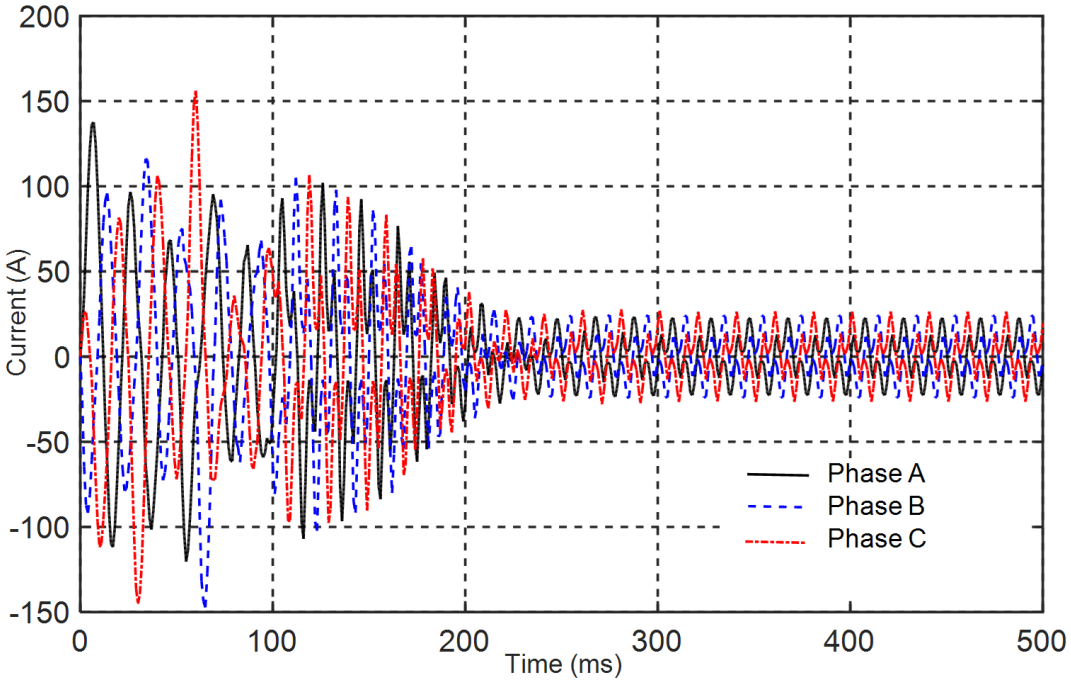

Fig. 33. Starting transient phase current response of the motor in 4-pole run

The transient analysis of speed, torque and input phase current is also done for eight-pole run and the results are as shown in Fig. 33, Fig. 34 and Fig. 35 respectively.

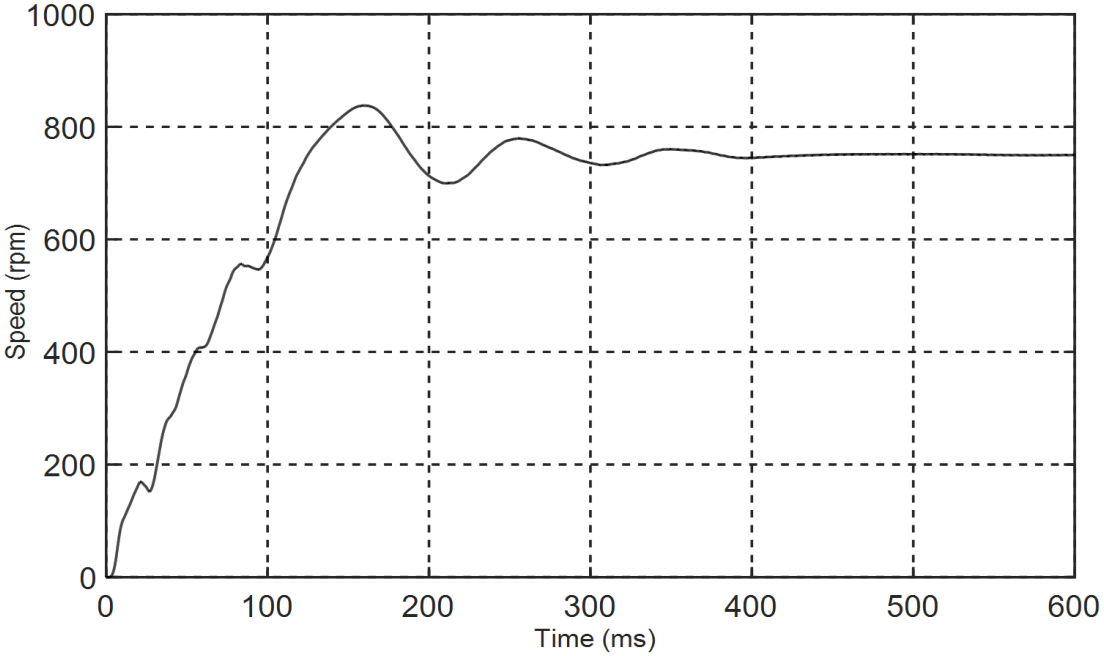

Fig. 34. Starting transient speed response of the motor in 8-pole run

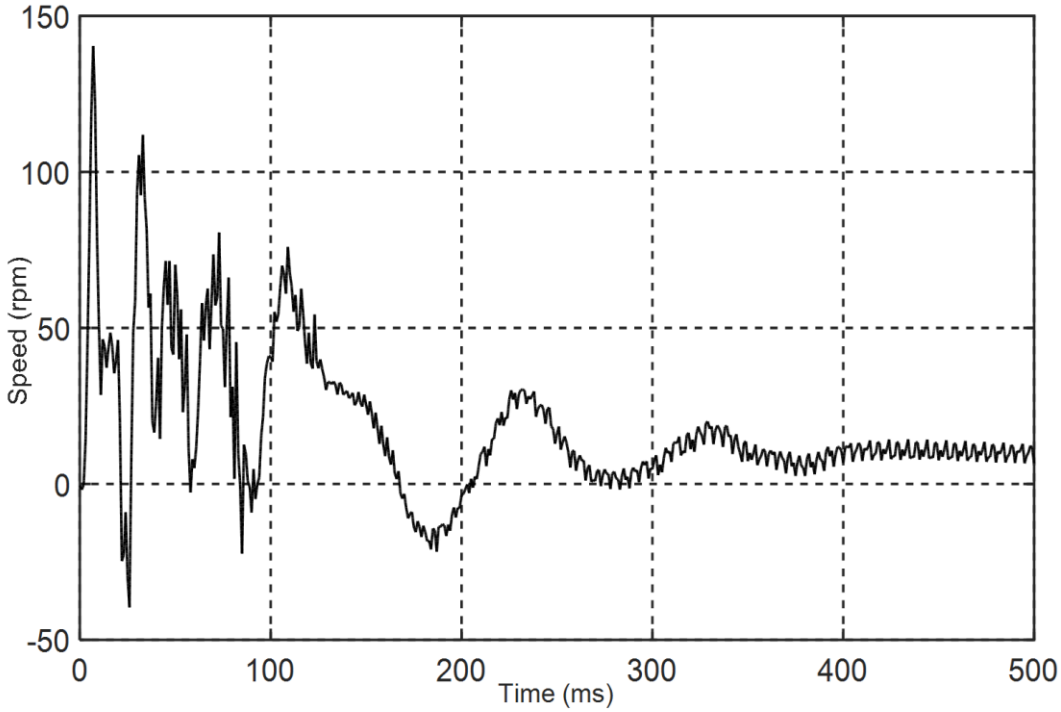

Fig. 35. Starting transient torque response of the motor in 8-pole run

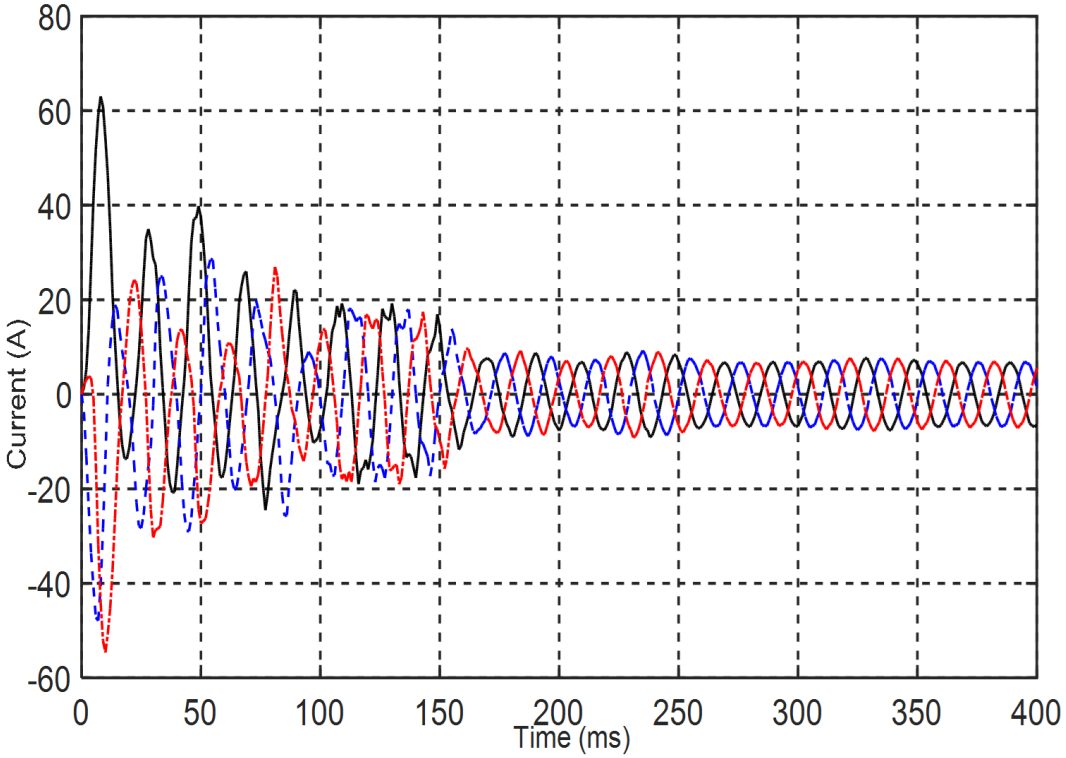

Fig. 36. Starting transient phase current response of the motor in 4-pole run

Fig. 37 and Fig. 38 shows the simulated speed response for for-pole and eight-pole run respectively at various load inertia. Similarly, Fig. 39 and Fig. 40 shows the simulated speed response for for-

pole and eight-pole run respectively at various starting load condition. From this analysis it is clear that the motor fails to synchronize at synchronous speed at higher load inertia and starting load torque.

Fig. 41 shows the transient response of the motor when it is first started with 8-pole stator winding and then switched to the 4-pole winding. It is to be noted that, dynamic behavior of the motor may be affected by the switching. The switching will create oscillation and the motor operation may be unstable unless the torque angle is close to nominal during the instant of switching [5].

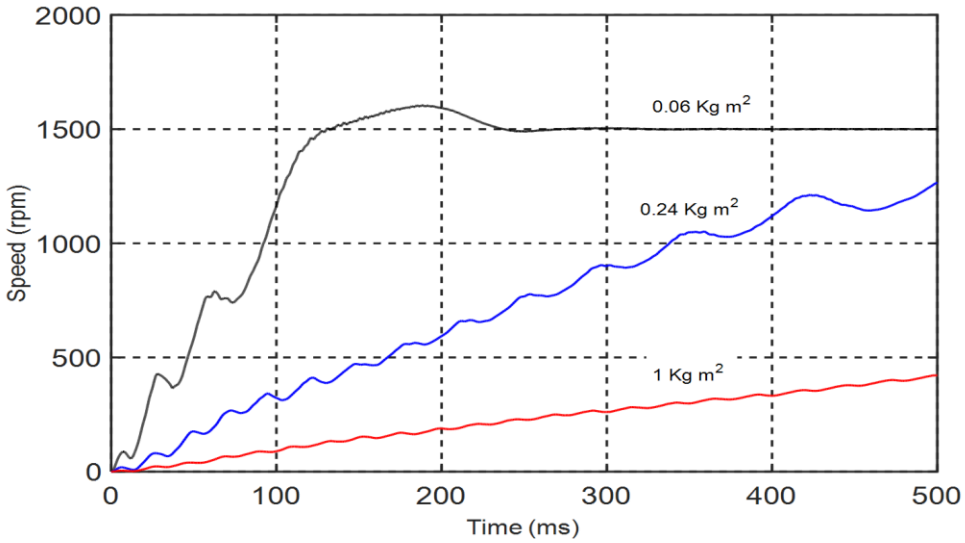

Fig. 37. Starting transient speed response for various inertia at 4 pole run

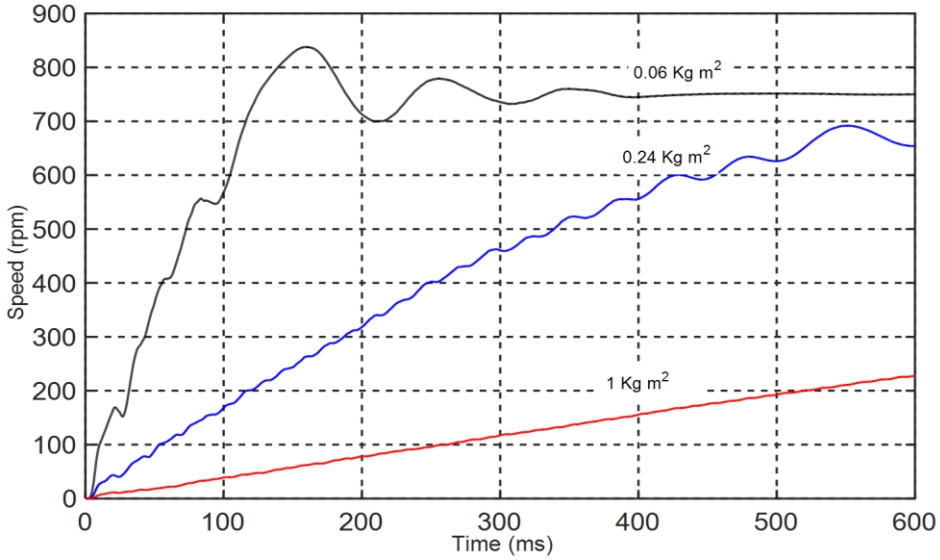

Fig. 38. Starting transient speed response for various inertia at 8 pole run

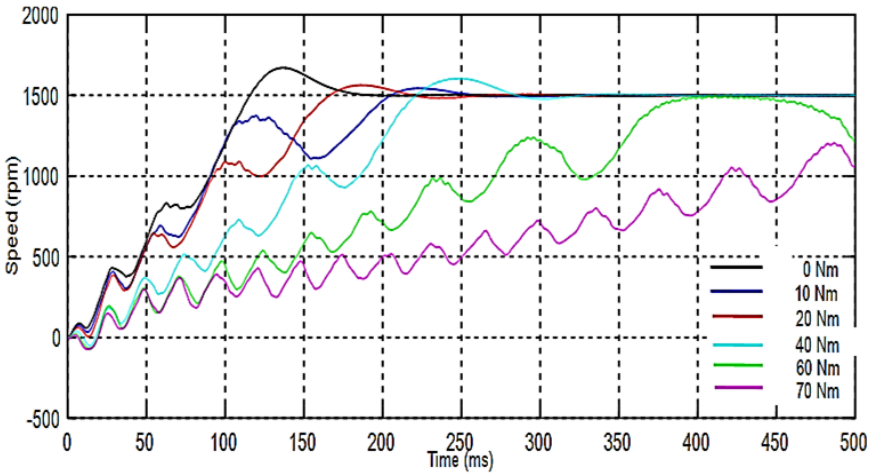

Fig. 39. Starting transient speed response for various starting load at 4 pole run

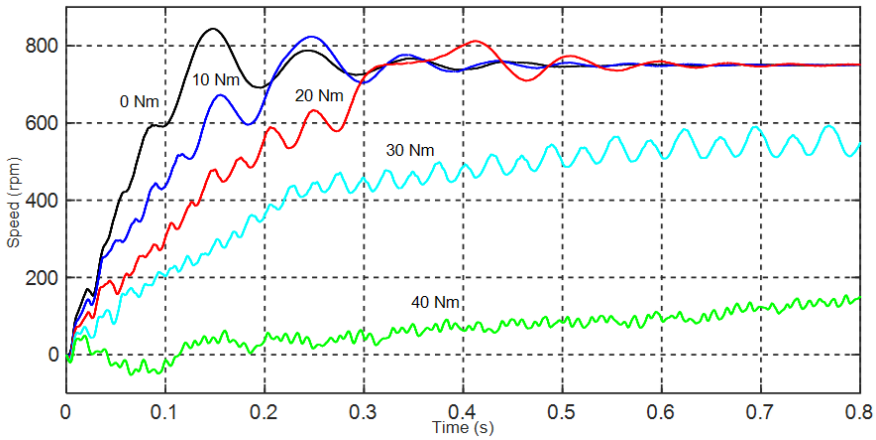

Fig. 40. Starting transient speed response for various starting load at 8 pole run

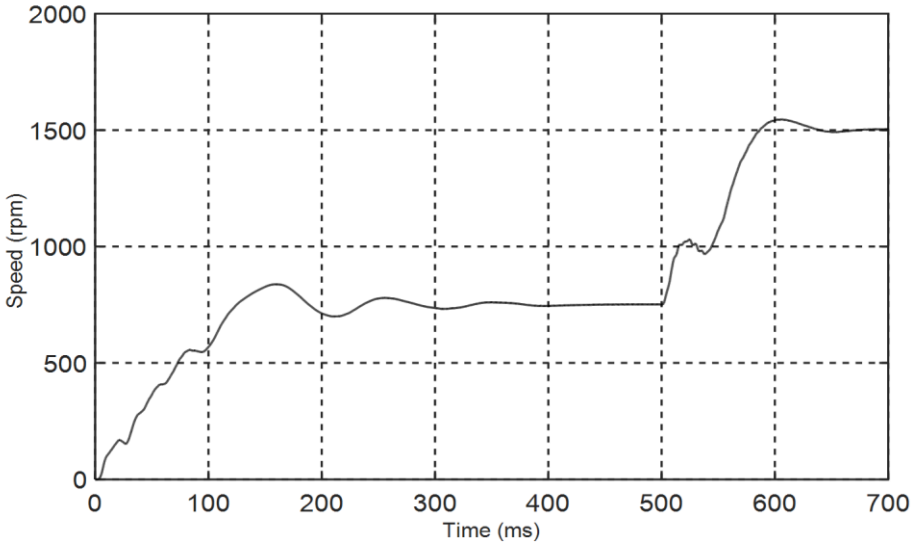

Fig. 41. Transient speed response of the motor switching from 8-pole to 4-pole run.

Fig 42 and Fig. 43 shows the efficiency of four-pole and eight-pole run respectively at different lamination factor of rotor core. The results show that as the lamination factor decreases the motor performs better due to low heat and eddy current loss. After certain lamination factor though the motor failed to start due to the fact that the flux lines couldn't travel through the rotor core.

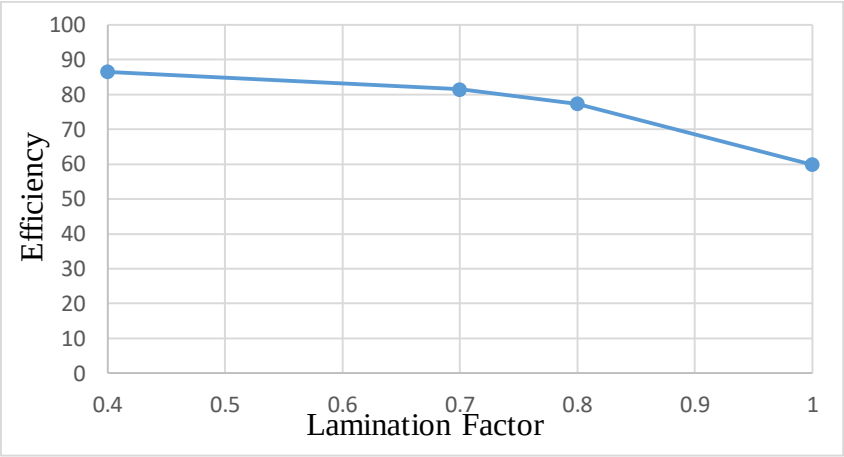

Fig. 42. Efficiency Vs. Lamination factor for 4-pole run

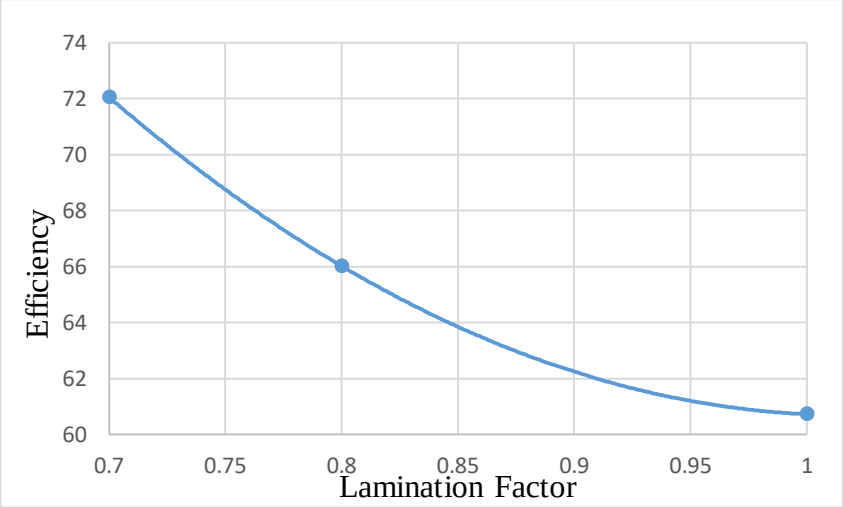

Fig. 43. Efficiency Vs. Lamination factor for 8-pole run

4.2 Scheme II: Dual Polarity Permanent Magnet Structure

4.2.1 Principle of Operation

In LSPM synchronous motor with this scheme the stator winding is made up of two independent winding with two different pole number (4/8). The windings are switched for high speed and low speed operations. The rotor is designed in such a way that it can incorporate pole number for both high speed as well as low speed operations. The permanent magnets in the rotor are arranged in such a way that the magnetic flux distribution is same to the resultant flux of two rotors with two different polarities.

Fig. 44 depicts the magnetic flux distribution in the air gap associated with each magnetic pole count to realize the rotor design with dual magnetic polarity (4/8 Magnetic poles). Fig. 45 shows the resultant flux for such arrangements. When seen from the four-pole run perspective the resultant flux is strengthening in one half and weakened in the other half under each pole.

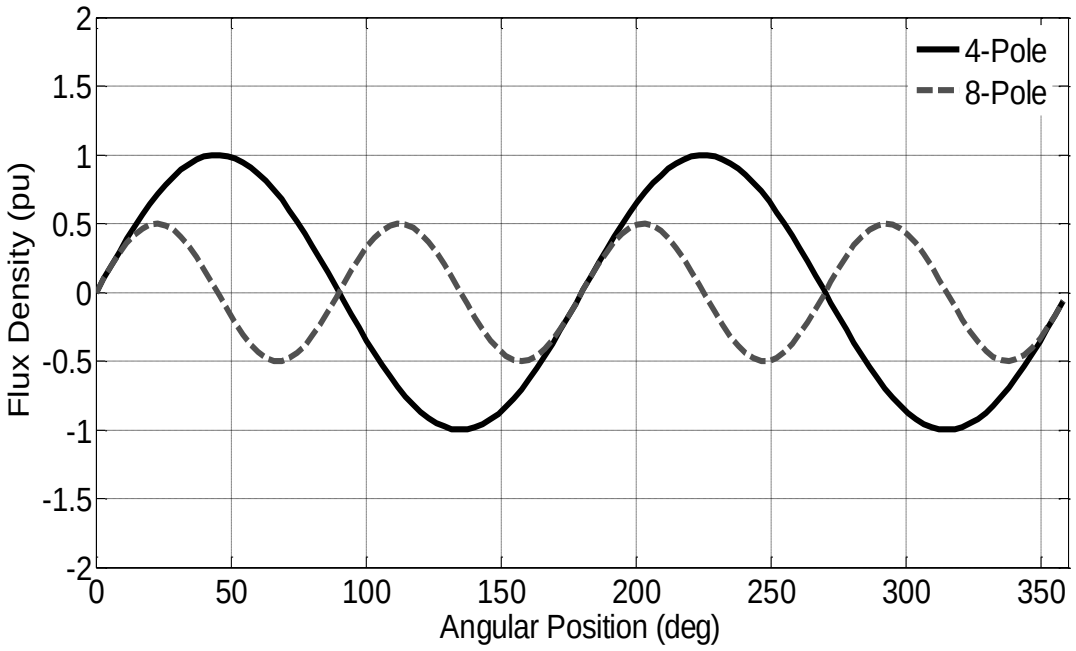

Fig. 44. The flux density distribution in the case of 4-pole and 8-pole rotor.

To achieve dual magnetic polarity, the rotor is designed to create the flux as shown in Fig. 45 and such flux distribution is achieved by reversing the magnetization direction of the adjacent PMs embedded in the rotor as shown in Fig 46(b). This stator and rotor arrangement is identical to the scheme I as shown in Fig. 46(a), the only difference being the reversed polarity of adjacent magnets.

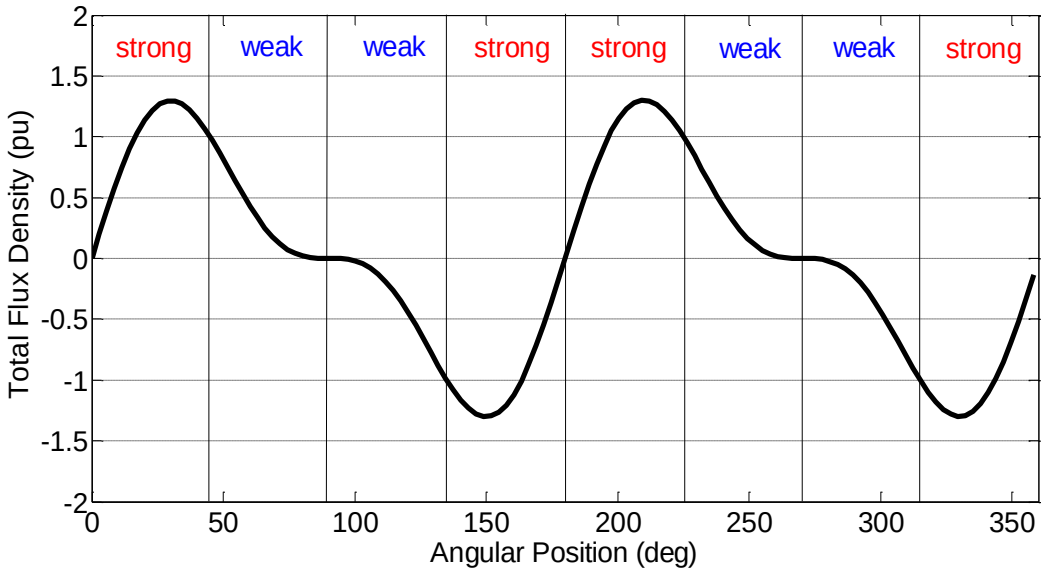

Fig. 45. The resultant flux density distribution of the 4-pole and 8-pole rotor (flux distribution in the proposed rotor design).

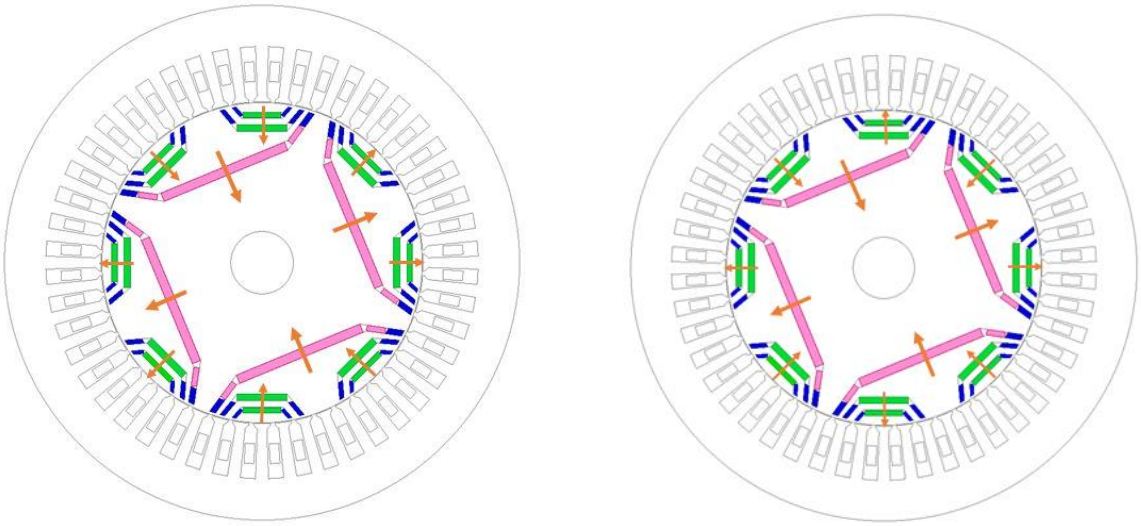

(a) (b)

Fig. 46. Schematic of the proposed motors(PM polarities are specified by arrows) (a) Scheme I (b) Scheme II.

4.2.2 Simulation and Results

4.2.2.1 Steady State Analysis

Fig. 47 and Fig. 48 shows the Back EMF induced in the four-pole and eight-pole armature (stator) windings. It is seen that the nature of the generated EMF is almost identical to sinusodial waveform. Between the two waveforms voltage induced in eight-pole winding has less number of harmonics and also has lower amplitude.

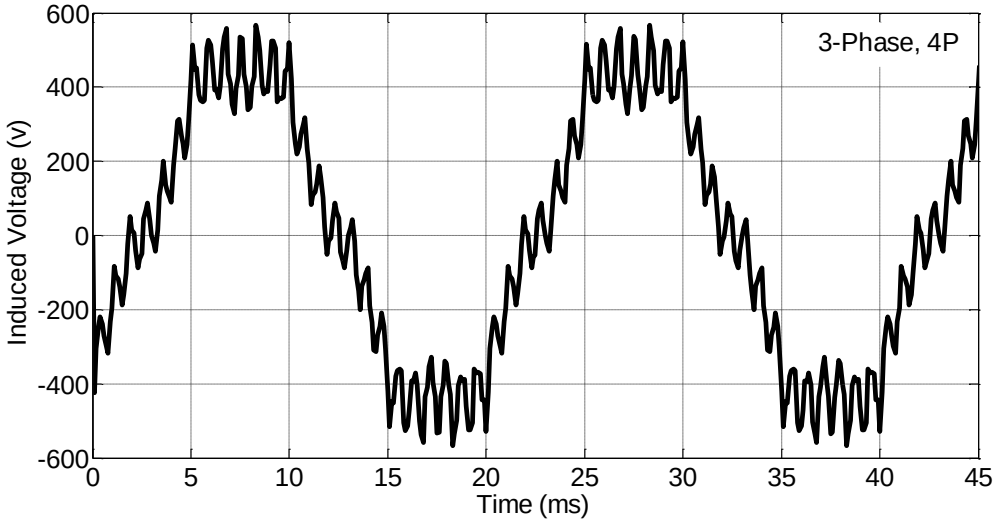

Fig. 47. The line to line back EMF induced in 4-pole windings.

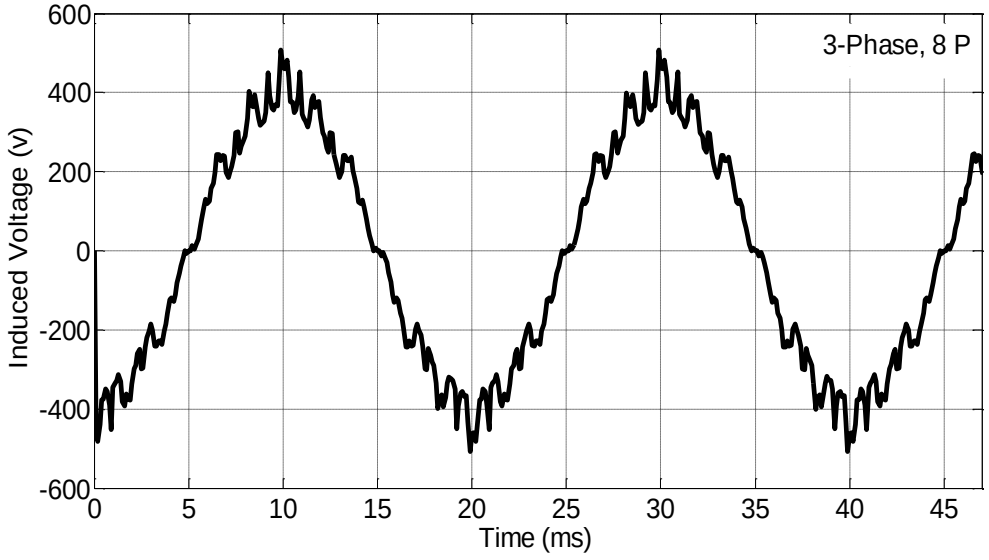

Fig. 48. The line to line back EMF induced in 8-pole windings.

At synchronous speed, the induction torque produced by the squirrel cage bars becomes zero. In this mode, according to the equation (36) the produced torque consists of two terms; reluctance torque and permanent magnet torque.

$$T_s = \frac{3p}{2\omega_s}.\frac{E_o U}{X_{ds}}\sin(\delta) + \frac{3p}{4\omega_s}.\frac{U^2(X_{ds}-X_{qs})}{X_{ds}.X_{qs}}sin(2\delta) \quad (36)$$

Where,

$p =$ number of poles

$\omega_s =$ synchronous angular velocity

$E_o =$ no load back EMF generated by the PMs

$X_{ds} =$ direct reactance at the synchronous frequency

$X_{qs} =$ quadrature reactance at the synchronous frequency

$T_s =$ synchronous torque

$U =$ input voltage

$\delta =$ torque angle

In both eight-pole and four-pole operation Permanent Magnet pole nature is dominant. In comparison to Scheme I, since Scheme two has permanent magnet pole also for low speed operation, torque is expected to increase significantly.

Variation of synchronous torque versus the rotor angle for four-pole and eight-pole operation is shown in Fig. 49 and Fig. 50 respectively. Although the torque is near sinusoidal, it is not completely sinusoid due to the presence of reluctance torque as explained by equation (36).

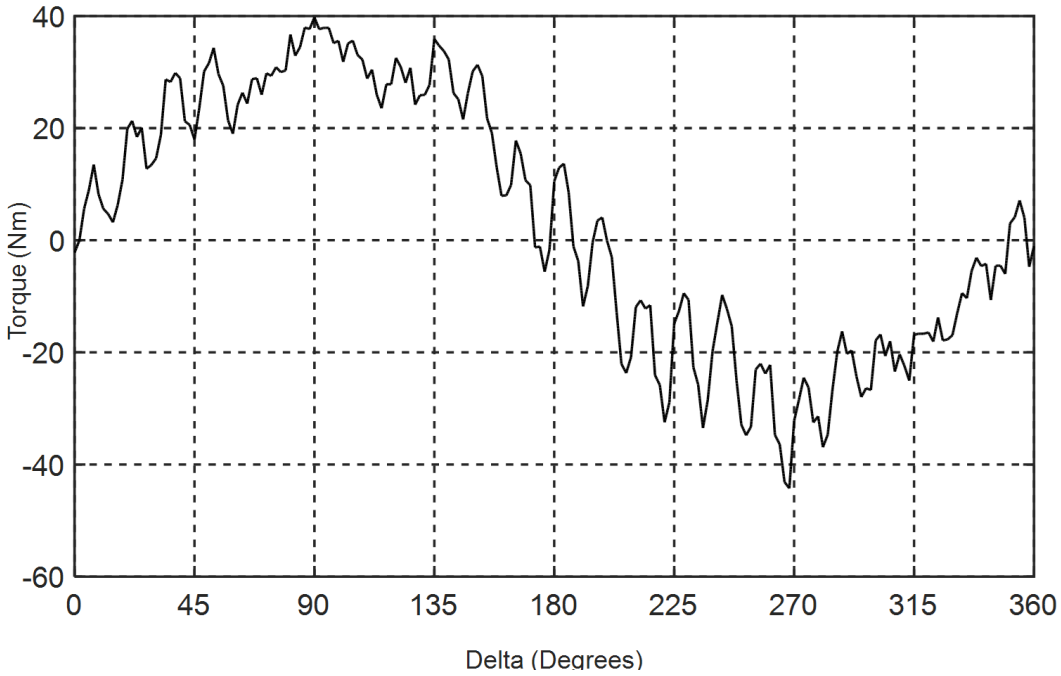

Fig. 49. Synchronous torque vs rotor angle in the 4-pole operating mode.

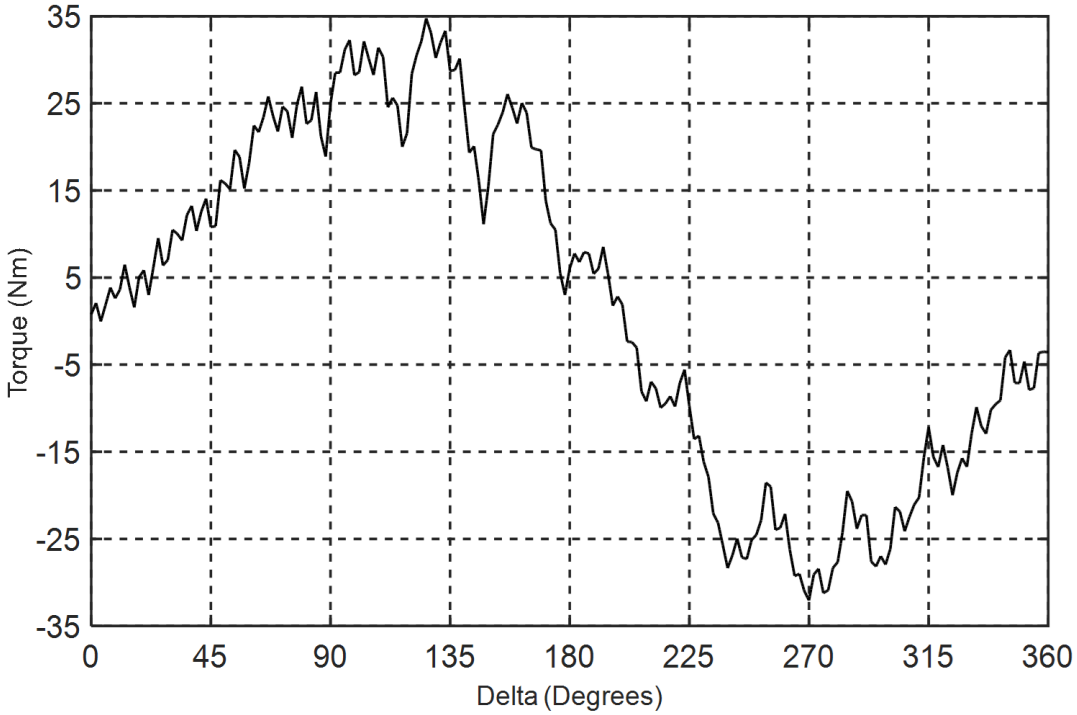

Fig. 50. Synchronous torque vs rotor angle in the 8-pole operating mode.

4.2.2.2 Transient Analysis

The proposed motor is started under a fan type load to examine the starting torque and synchronization capability. For a fan type load, the load torque is proportional to the square of motor speed and the nature of the torque is shown in Fig. 51. Based on the torque Vs. sped nature, the load torque at maximum speed of 1500 RPM is 40 Nm. For all the analysis applied line to line voltage is 380V.

Fig. 52 depicts the speed-time response of eight-pole run of the motor. From the graph it can be clearly stated that, the motor successfully starts and reaches the steady state synchronous speed of 750 RPM. Fig. 53 and Fig. 54 shows the torque-time and stator phase current-time response respectively for eight-pole run.

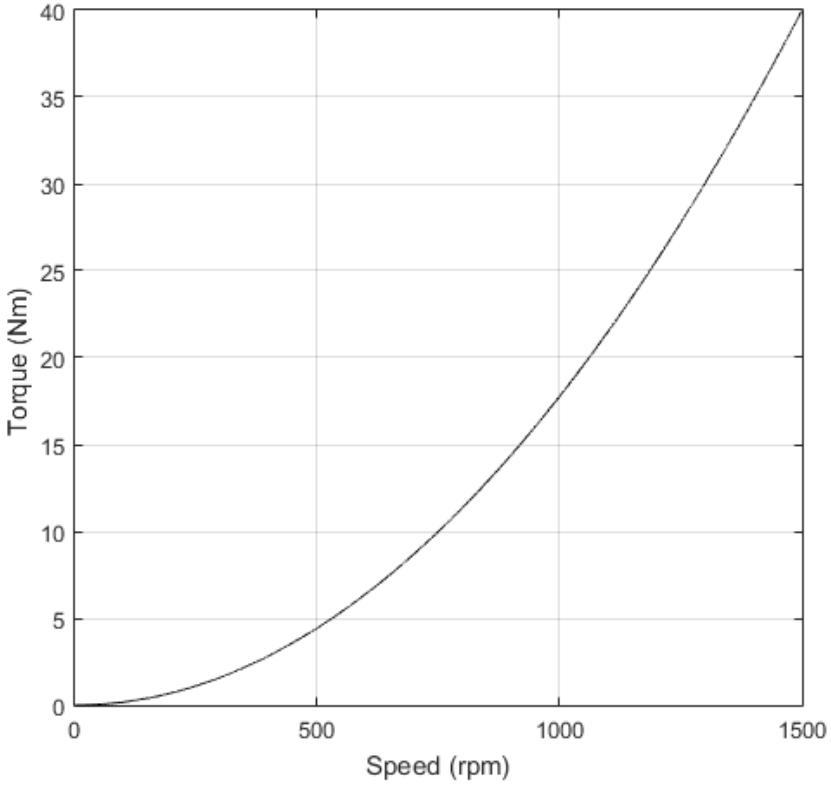

Fig. 51. Speed Vs. Torque Response

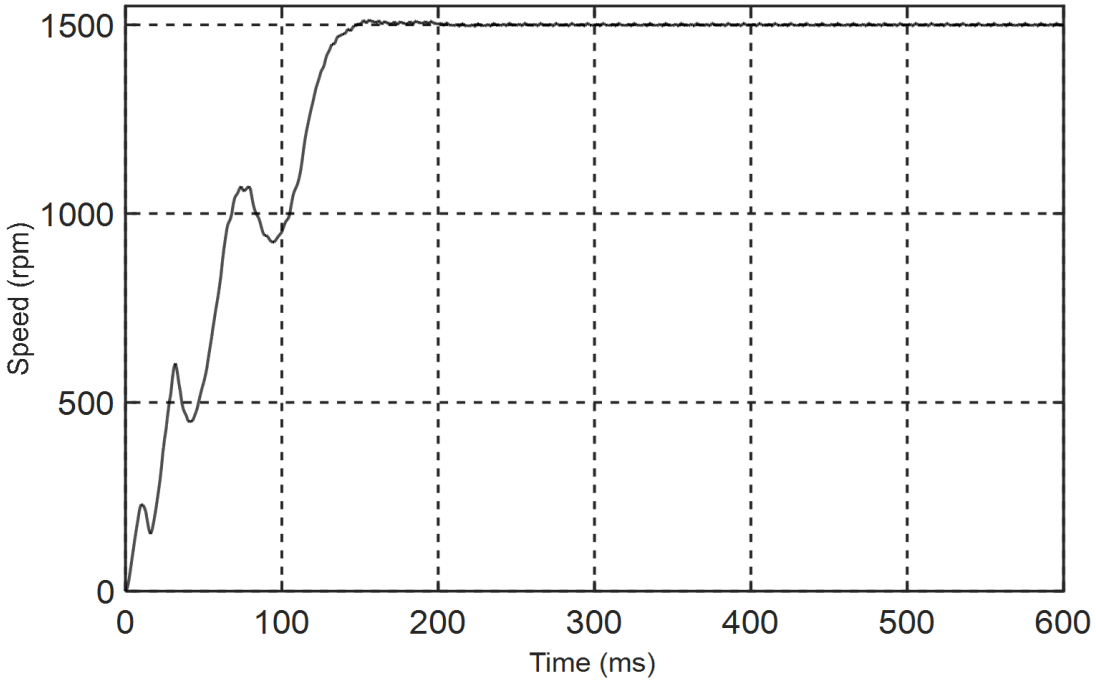

Fig. 52. Transient speed response in 8-pole run.

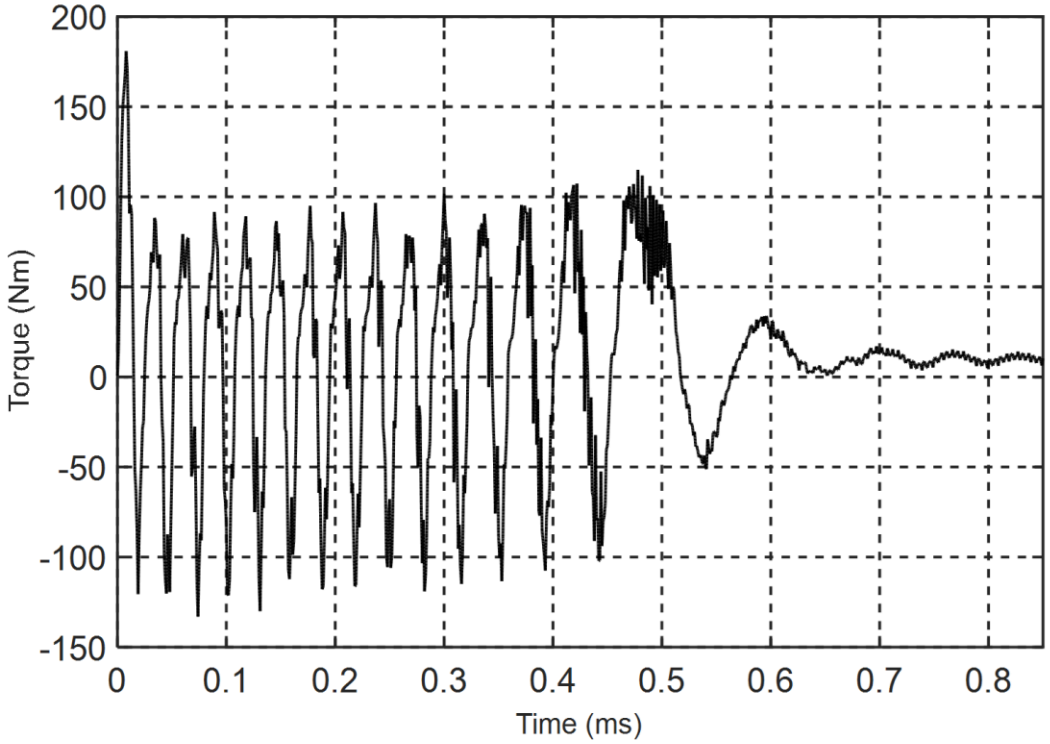

Fig. 53. Transient torque characteristic in 8-pole run.

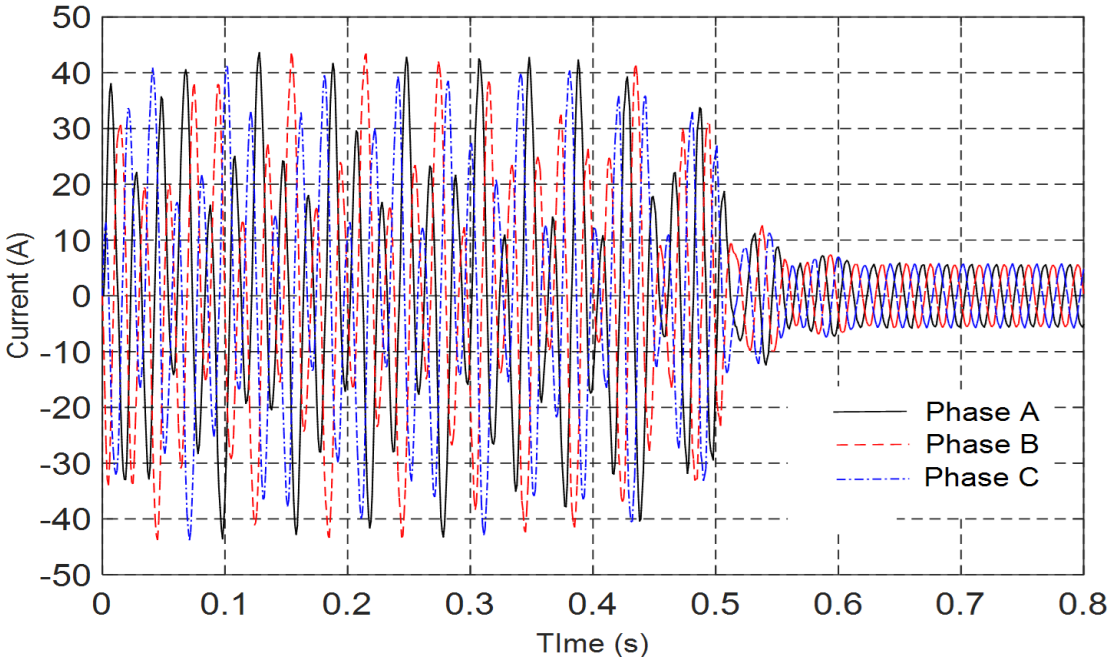

Fig. 54. Transient input current characteristic in 8-pole run.

It's seen that the motor stabilizes itself after some oscillation. These procedures are repeated for four-pole run and Fig. 55, Fig. 56 and Fig. 57 shows the speed-time, torque-time and stator phase current-time response for four-pole run respectively.

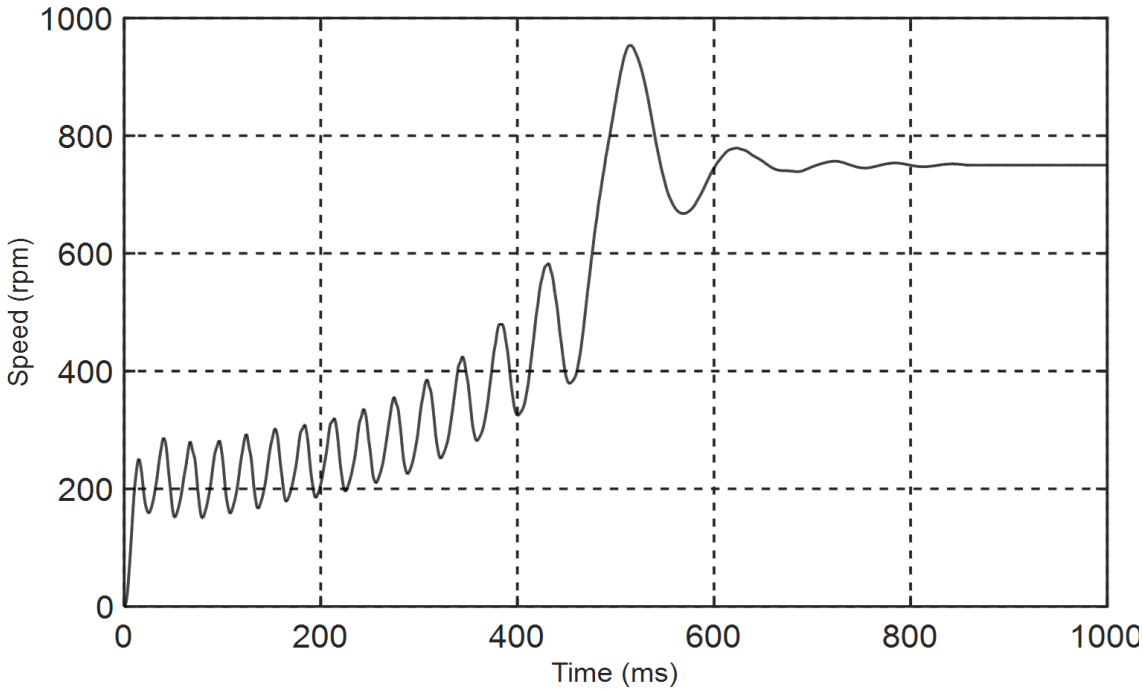

Fig. 55. Transient Speed characteristic in 4-pole run.

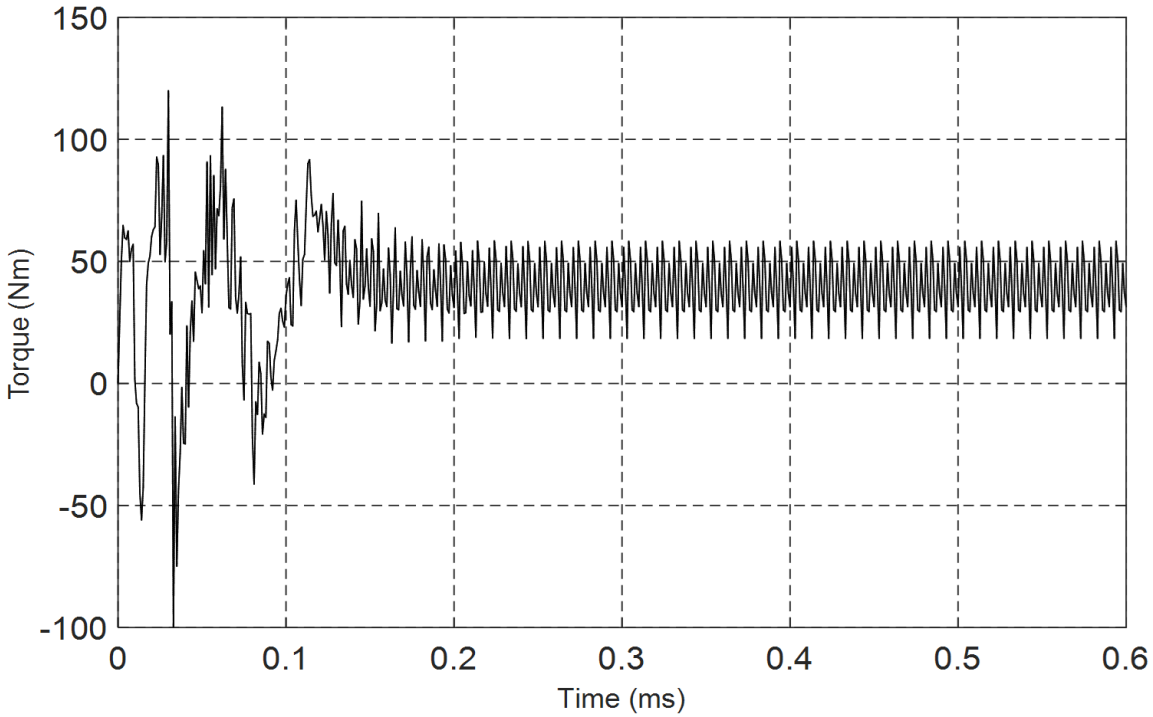

Fig. 56. ransient torque characteristic in 4-pole run.

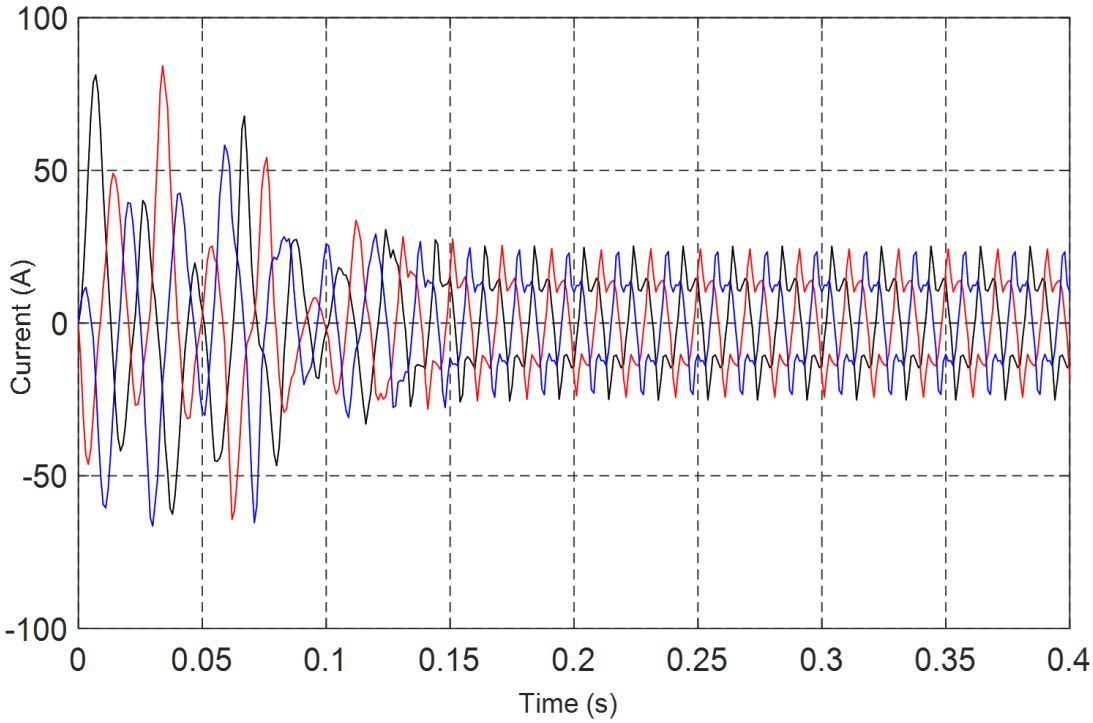

Fig. 57. Transient input 3-phase current characteristic in 4-pole run.

Fig. 58 and Fig. 59 depicts the speed-time response under various load inertia condition for four-pole run and eight-pole run respectively. Whereas, Fig. 60 and Fig. 61 shows the speed-time response under various load torque conditions. From the four simulations it's clear that the motor fails to start at higher initial load inertia or load torque conditions.

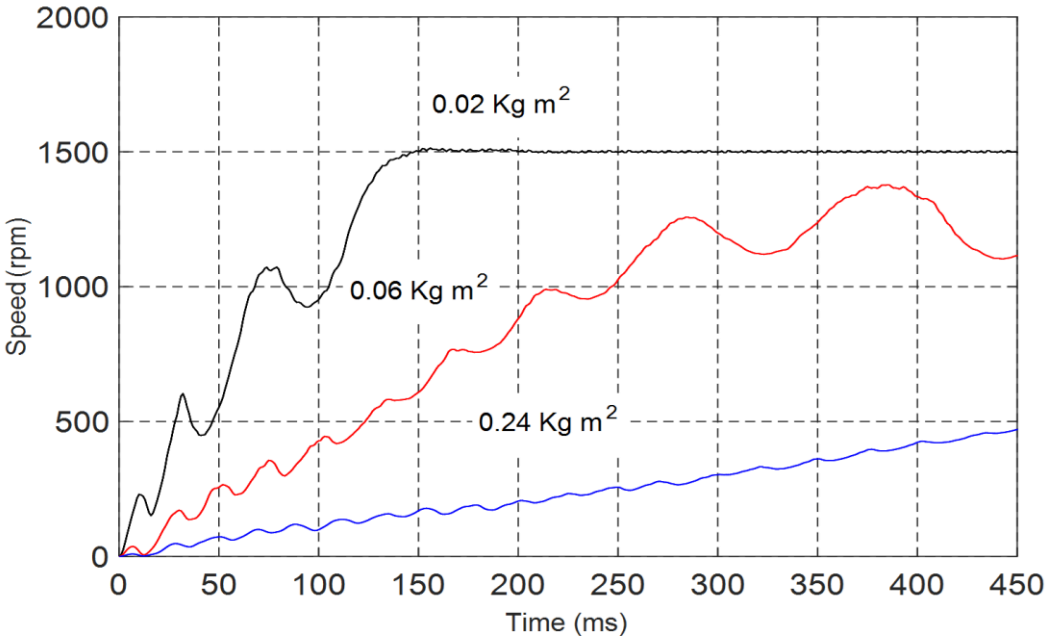

Fig. 58. Starting transient speed response for various load inertia for 4 pole run

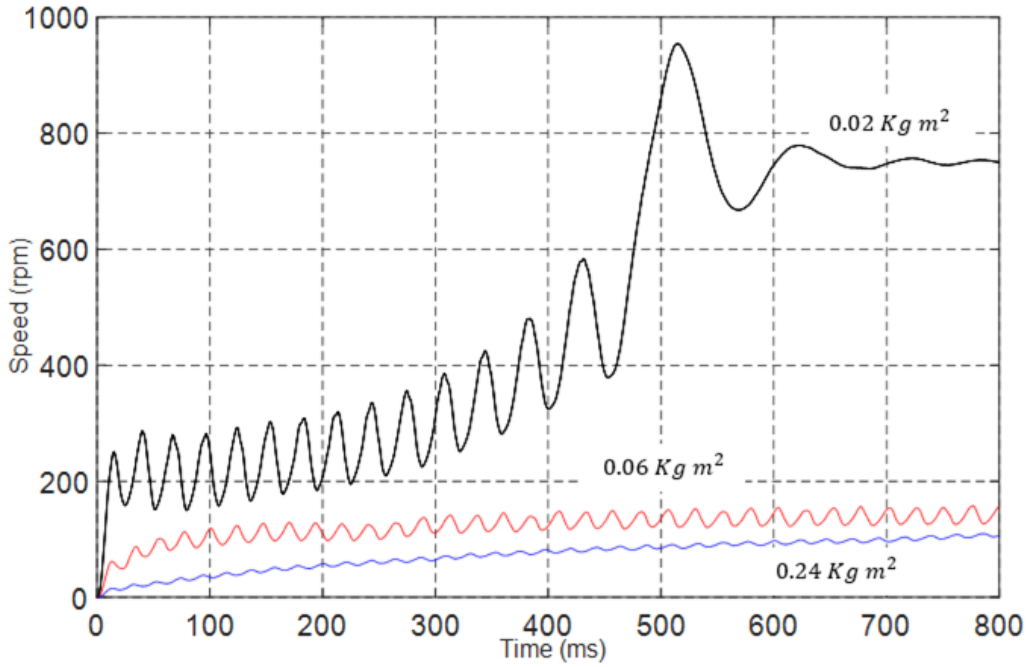

Fig. 59. Srting transient speed response for various load inertia for 8 pole run

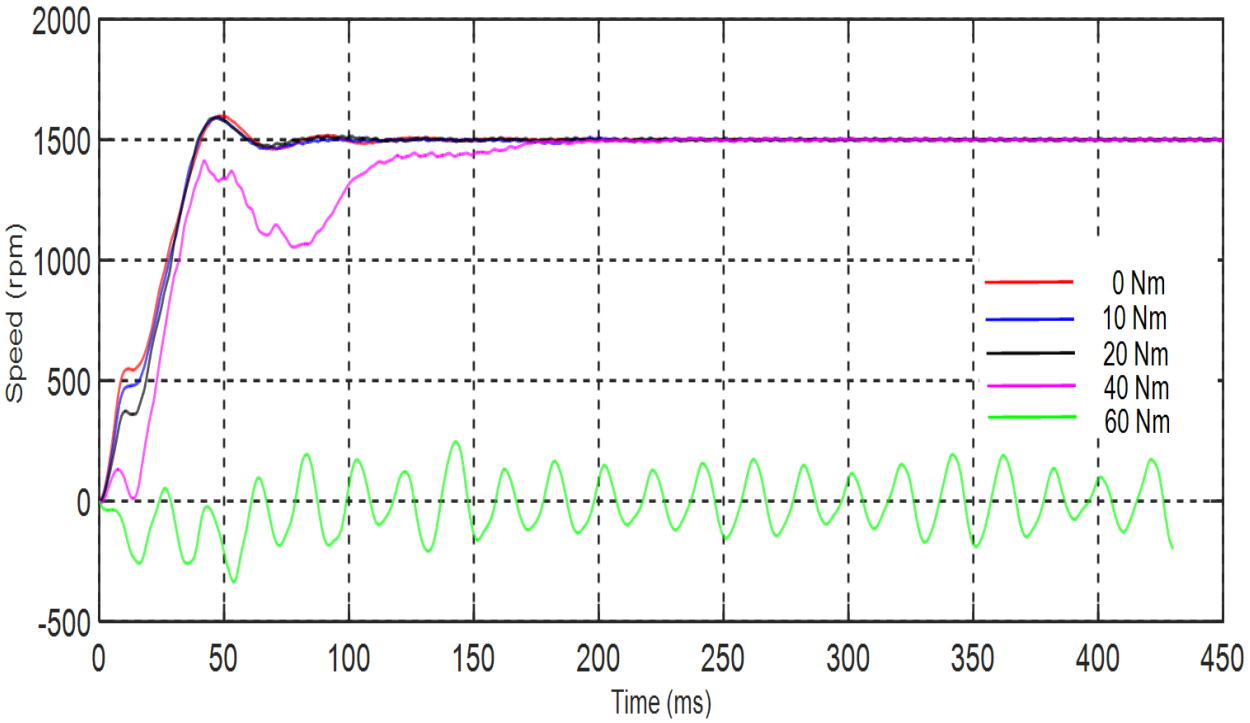

Fig. 60. Starting transient speed response for various load torque for 4 pole run.

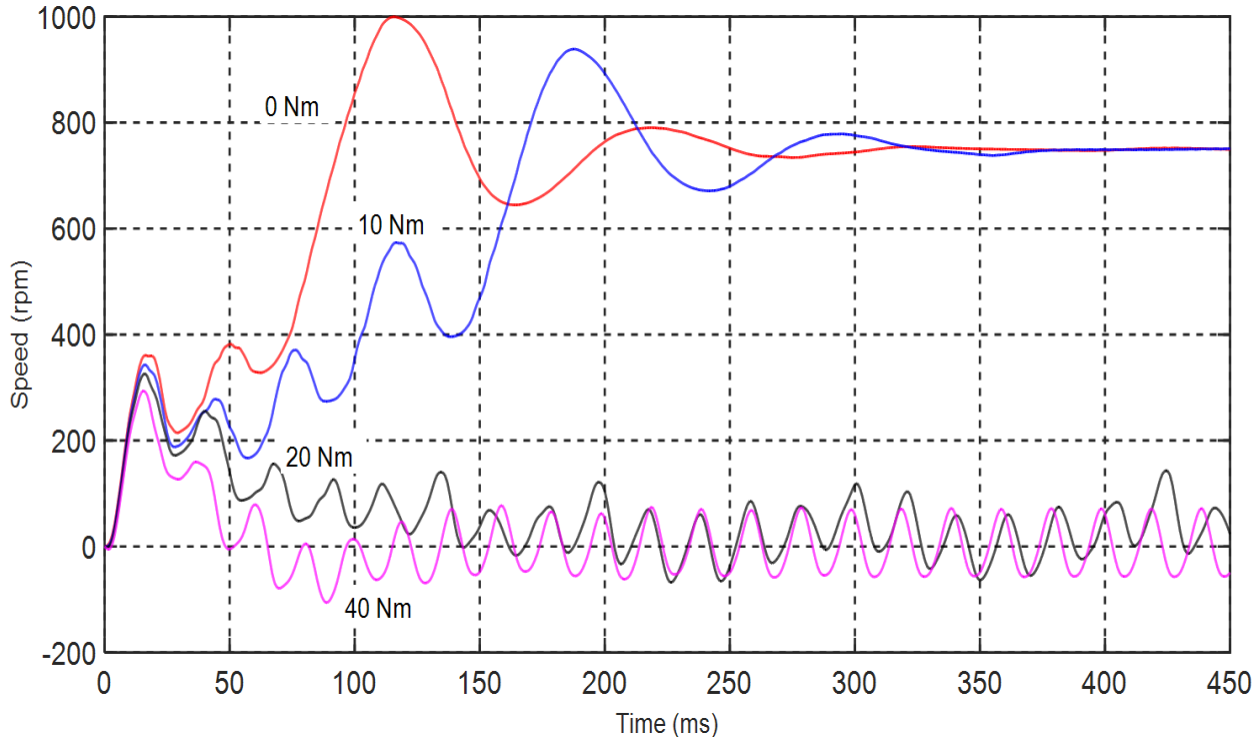

Fig. 61. Starting transient speed response for various load torque for 8 pole run.

Fig 62 and Fig. 63 shows the efficiency of four-pole and eight-pole run respectively at different lamination factor of rotor core. The results show that as the lamination factor decreases the motor performs better due to low heat and eddy current loss. After certain lamination factor though the motor failed to start due to the fact that the flux lines couldn't travel through the rotor core.

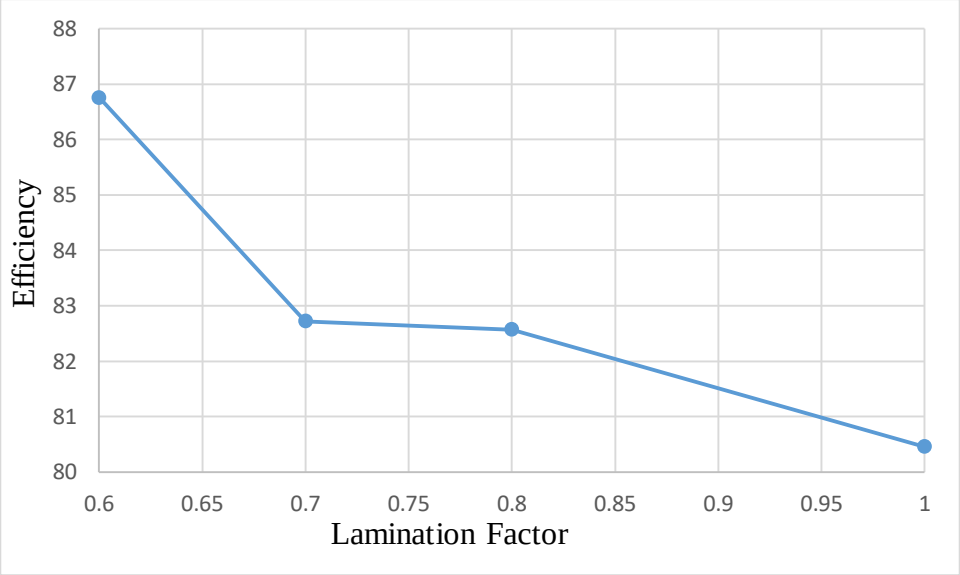

Fig. 62. Efficiency Vs. Lamination factor for 4-pole run

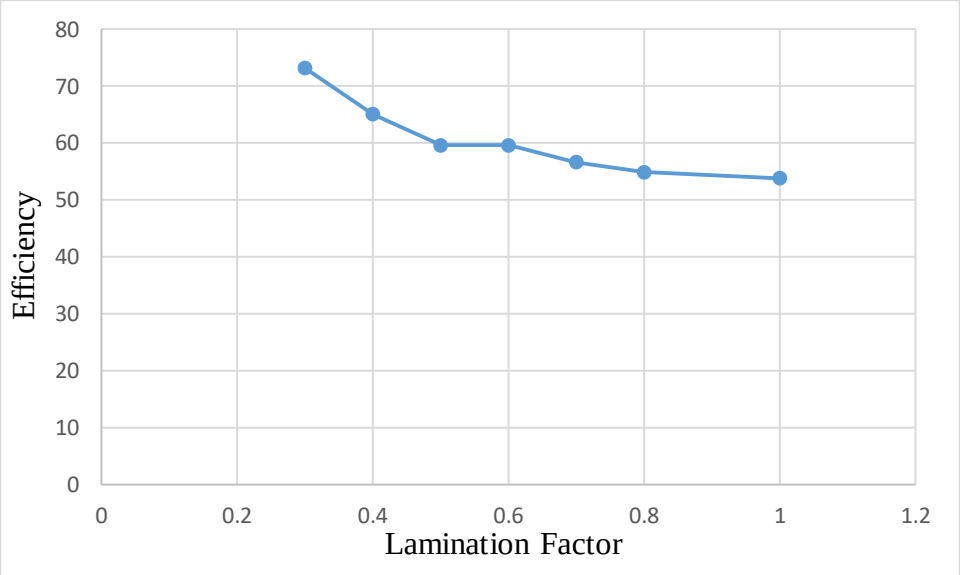

Fig. 63. Efficiency Vs. Lamination factor for 8-pole run

Chapter 5
Conclusion

This thesis presents analyses and verification of two different schemes for dual speed LSPM Synchronous Motor using 3-D FEA. Scheme I involves motor design based on permanent magnet structure as well as reluctance structure. The stator consists of two independent pole windings (4/8) whereas the rotor consists of four-pole permanent magnet configuration superimposed with eight-pole reluctance configuration. This design enables the motor to run at high speed as a synchronous permanent magnet motor and at low speed as synchronous reluctance motor. Scheme II involves a new design of rotor in which both the high speed and low speed mode works based on synchronous permanent magnet configuration.

Comparing steady state Torque Vs. Power angle response of both the motors, the maximum synchronous torque at high speed run (four-pole) was same in both the case but for low speed run at eight-pole run based on synchronous reluctance nature the maximum synchronous torque was significantly lower than that of eight-pole synchronous permanent magnet based nature of scheme II.

Similarly, Back EMF for both pole operation of Scheme II was more sinusoidal than that of four-pole operation of Scheme I. Efficiency for both the motors were approximately the same for four-pole operation at 0.7 lamination factor but for eight-pole operation the efficiency of Scheme II was lower than Scheme I. But for both the motors efficiency increased while laminated steel core was used instead on solid steel core.

The motors were initially designed for fan type load, meaning the initial load would be zero and increase proportional to square of speed but simulations were also done with various starting load. Both scheme started and synchronized at high speed when load up to 40 Nm was used but for low

speed run although Scheme I started with load torque up to 20Nm, Scheme II could only start with load torque up to 10 Nm.

5.1 Future Scope of the study

The proposed motor designs can be improved in future by performing motor design optimization. Also, till now no study has been conducted to compare the difference between the proposed and conventional motors which can be done in future. Furthermore, applying variable frequency drive the distant speed change using pole switching can be accompanied with local speed change. This helps the design to operate in wider speed range. Development of the motor prototype for the experimental testing can be done and the experimental results can be compared with the simulated results.

References

[1] Z. Bingyi, L. Bingxue, F. Guihong, and Z. Fuyu, "Starting Performance Analysis of Single Phase Line Start Permanent Magnet Motor", IEEE International conference on Mechatronics and Automation, China, pp. 2883-2888, 2007.

[2] A. Hassanpour Isfahani, and S. Vaez-Zadeh, "Line Start Permanent Magnet Synchronous Motors: Challenges and Opportunities", Elsevier Journal on Energy, vol.34, no. 11, pp. 1755-1763, 2009.

[3] T. Ding, N. Takorabet, F.M. Sargos, and X. Wang, "Design and Analysis of Different Line-Start PM Synchronous Motors for Oil-Pump Applications", IEEE Transactions, Magnetics, vol. 45, no. 3, pp. 1816-1819, 2009.

[4] A. Damaki Aliabad, M. Mirsalim, and N. Farrokhzad Ershad, "Line-Start Permanent-Magnet Motors: Significant Improvements in Starting Torque, Synchronization, and Steady-State Performance", IEEE Transactions, Magnetics, Vol. 46 , no. 12, pp. 4066 – 4072, 2010.

[5] A. Damaki Aliabad, and M. Mirsalim, "Analytic Modeling and Dynamic Analysis of Pole-Changing Line-Start Permanent Magnet Motors", IET Electric Power Applications, Vol. 6, no. 3, pp. 149-155, 2012.

[6] N. Farrokhzad Ershad, M. Mirsalim, and A. Damaki Aliabad, "Line-Start Permanent Magnet Motors: Proper Design for Pole-Changing Starting Method", IET Electric Power Applications, Vol. 7, no. 6, pp. 470-476, 2013.

[7] K. Kurihara, and M.A. Rahman, "High-Efficiency Line-Start Interior Permanent-Magnet Synchronous Motors", IEEE Transactions, Industry Applications, vol. 40, no. 3, pp. 789-796, 2004.

[8] H. Lee, J. P. Hong, and J. H. Lee, “Optimum design criteria for maximum torque and efficiency of a line-start permanent-magnet motor using response surface methodology and finite element method,” *IEEE Trans. Magn.*, vol. 48, no. 2, pp. 863–866, Feb. 2012.

[9] T. J. E. Miller, "Synchronization of Line-Start Permanent-Magnet AC Motors," in *IEEE Transactions on Power Apparatus and Systems*, vol. PAS-103, no. 7, pp. 1822-1828, July 1984.

[10] R. W. Wieseman, “A two-speed salient-pole synchronous motor,” *Trans. Amer. Inst Elect. Eng.*, vol. XLIV, pp. 436–446, 2009.

[11] J. Bialik and J. Zawilak, “Vibration modeling of the two-speed, large power, synchronous motor,” in Proc. IEEE Int. Symp. Diagnostics Electri. Mach., Power Elect. Drives, 2007, pp. 173–177.

[12] V. Ostovic, “Pole-changing permanent-magnet machines”, *IEEE Transactions, Industry Applications*, vol. 38, no. 6, pp. 1493-1499, Dec. 2002.

[13] K. Sakai, and H. Hashimoto, “Permanent magnet motors to change poles and machine constants”, *International Conference, Electrical Machines (ICEM),* pp. 435 – 440, 2012.

[14] F. J. Haddad Kalluf, L. N. Tutelea, I. Boldea and A. Espindola, “2/4-POLE Split-Phase Capacitor Motor for Small Compressors: A Comprehensive Motor Ch22aracterization”, *IEEE Transactions, Industry Applications,* Vol. 50, no. 1, pp. 356 – 363, 2014.

[15] V. D. Toro, “Electric machines and Power System”, Prentice-Hall, Englewood Cliffs, N.J., 1985

[16] A.E. Fitzgerald, and C. Kingsley, “Electric Machinery”, McGraw-Hill, New York, 1952

[17] A.E. Fitzgerald, C. Kingsley, and S.D. Umans, “Electric Machinery,6th Ed.”, McGraw-Hill, New York, 2003

[18] M. Liwschitz-Garik, and C. Whipple, “Alternating-Current Machinery”, Princeton, N.J., 1961

[19] G. McPherson, “An Introduction to Electrical Machines and Transformers”, Wiley, New York, 1981

[20] E. H. Werninck, “Electric Motor Handbook”, McGraw-Hill Book Company, London, 1978

[21] A. N. Chaston., “Electric Machinery. Reston”, Reston Publishing, 1986

[22] G. R. Slemon, A. Straughen, “Electric Machines”, Addison-Wesley Publishing, 1980

[23] S. J. Chapman, “Electric Machines Fundamentals, 5th Ed.”, McGraw-Hill, New York, 2012

[24] D. J. Griffiths, “Introduction to Electrodynamics, 2nd Ed.”,Prentice Hall, 1989

VITA

Bikrant Poudel was born in 1991 in Kathmandu, Nepal. He finished his Bachelor in Electronics and Communication Engineering from Tribhuvan University on December of 2013. After which he worked as information technology Officer at Government of Nepal, District Development Committee. He also worked as robotics and embedded system trainer. In 2015 he came to University of New Orleans to pursue his Masters of Science in Electrical Engineering concentration. He is currently a candidate for the degree of Masters of Science in Electrical Engineering which will be awarded in December 2017.